



## Review article

Tetraalkylammonium salts (TAS) in solar energy applications – A review on *in vitro* and *in vivo* toxicityN.M. Mustafa<sup>a</sup>, F.N. Jumaah<sup>b</sup>, N.A. Ludin<sup>a</sup>, M. Akhtaruzzaman<sup>a,c</sup>, N.H. Hassan<sup>d,e</sup>, A. Ahmad<sup>d,e,f</sup>, K.M. Chan<sup>g</sup>, M.S. Su'ait<sup>a,\*</sup><sup>a</sup> Solar Energy Research Institute (SERI), Universiti Kebangsaan Malaysia, 43600, Bangi, Selangor, Malaysia<sup>b</sup> Department of Materials & Life Sciences, Sophia University, 7-1 Kioi-cho, Chiyoda-ku, Tokyo, 102-8554, Japan<sup>c</sup> Department of Chemistry, Faculty of Science, Islamic University of Madinah, Madinah, Saudi Arabia<sup>d</sup> Department of Chemical Sciences, Faculty of Science and Technology, Universiti Kebangsaan Malaysia, 43600, Bangi, Selangor, Malaysia<sup>e</sup> Battery Technology Research Group (UKMBATT), Polymer Research Centre (PORCE), Faculty of Science and Technology, Universiti Kebangsaan Malaysia, 43600, Bangi, Selangor, Malaysia<sup>f</sup> Department of Physics, Faculty of Science and Technology, Universitas Airlangga, Jl. Mulyorejo, Surabaya, 60115, Indonesia<sup>g</sup> Product Stewardship and Toxicology, Group Health, Safety and Environment (GHSE), Petrolia Nasional Berhad (PETRONAS), 50088 Kuala Lumpur, Malaysia

## ARTICLE INFO

## Keywords:

Energy  
Ionic liquids  
Solar cell  
Tetraalkylammonium  
Toxicity

## ABSTRACT

Tetraalkylammonium salt (TAS) is an organic salt widely employed as a precursor, additive or electrolyte in solar cell applications, such as perovskite or dye-sensitized solar cells. Notably, Perovskite solar cells (PSCs) have garnered acclaim for their exceptional efficiency. However, PSCs have been associated with environmental and health concerns due to the presence of lead (Pb) content, the use of hazardous solvents, and the incorporation of TAS in their fabrication processes, which significantly contributes to environmental and human health toxicity. As a response, there is a growing trend towards transitioning to safer and biobased materials in PSC fabrication to address these concerns. However, the potential health hazards associated with TAS necessitate a thorough evaluation, considering the widespread use of this substance. Nevertheless, the overexploitation of TAS could potentially increase the disposal of TAS in the ecosystem, thus, posing a major health risk and severe pollution. Therefore, this review article presents a comprehensive discussion on the *in vitro* and *in vivo* toxicity assays of TAS as a potential material in solar energy applications, including cytotoxicity, genotoxicity, *in vivo* dermal, and systemic toxicity. In addition, this review emphasizes the toxicity of TAS compounds, particularly the linear tetraalkyl chain structures, and summarizes essential findings from past studies as a point of reference for the development of non-toxic and environmentally friendly TAS derivatives in future studies. The effects of the TAS alkyl chain length, polar head and hydrophobicity, cation and anion, and other properties are also included in this review.

\* Corresponding author. Solar Energy Research Institute (SERI), Universiti Kebangsaan Malaysia, 43600, Bangi, Selangor, Malaysia.  
E-mail address: [mohdsukor@ukm.edu.my](mailto:mohdsukor@ukm.edu.my) (M.S. Su'ait).

<https://doi.org/10.1016/j.heliyon.2024.e27381>

Received 27 July 2023; Received in revised form 28 February 2024; Accepted 28 February 2024

Available online 13 March 2024

2405-8440/© 2024 The Authors. Published by Elsevier Ltd. This is an open access article under the CC BY-NC license (<http://creativecommons.org/licenses/by-nc/4.0/>).

## 1. Introduction

Organic salts, also known as an engineered salt due to their flexible behaviour, are simple cation-anion mixtures that are formed by altering the ionic species and the functional groups in their organic chemical structure that may be composed of a combination of organic cations such as carbon, nitrogen, phosphorus and/or sulphur based and inorganic or organic polyatomic anions [1]. Tetraalkylammonium salts (TAS) are among the most frequently used quaternary ammonium salts in various industries and academia due to their unique physical and chemical properties, exceptional stability, tuneable properties and surface activity [2,3]. These quaternary ammonium salt structures exhibit a tripartite classification, distinguishing itself into ionic liquids (ILs), liquid crystals (LCs) or plastic crystals (PCs) based on nuanced considerations of both chemical structure and thermal behaviour [4]. It was discovered that cationic species have a considerable impact on the toxicity of TAS [5]. In contrast, anionic species only influence the physical characteristics of these substances, such as the melting point or viscosity [6]. In this review, our focus is on the functionality of TAS in the application of solar cells and its toxicity towards the environment. To date, TAS is widely used in the solar cell industry [7] as an electrolyte [7,8], synthesis reactant [9] and catalyst for chemical reactions [10], as a corrosion inhibitor [11], and a medium for electrodeposition of metals [12,13]. TAS also has been used in other fields such as anticancer [14], antimicrobial [14,15] as well as dental restoration material [16]. In addition, recent studies have demonstrated the potential use of TAS as precursors, additives, solvents, interfacial layers, and protective layers to enhance the power conversion efficiency (PCE) in perovskite solar cells (PSCs) [17–20].

Apart from lead (Pb) toxicity in PSCs, TAS cause a health hazard attention as well. In view of the widespread utilization of TAS, there is a strong need to evaluate the toxicity level of TAS in the best interest to preserve public health and prevent unfavourable impacts on the environment. Investigation of the level of toxicity of TAS is also critical so that the production disposal method of TAS can be carried out sustainably and safely. In the last 15 years, a collection of studies and review papers on the toxicity of TAS have been published to highlight the possible hazards of moderate-to-highly toxic TAS in industrial applications and identify efficient approaches to modify their chemical structures to minimize their toxicity. Thus, this review aimed to examine the *in vitro* and *in vivo* toxicity assays of TAS, including cytotoxicity, genotoxicity, *in vivo* dermal, and systemic toxicity, following its potential use in solar energy applications. It is essential to highlight that the focus of the review centres on quaternary ammonium ions, with a specific emphasis on the detailed examination of tetraalkylammonium ions  $[N_{R_n}^+][X^-]$ .

### 1.1. Structure of TAS

Generally, TAS contains positively charged nitrogen atoms with the chemical formula of  $[N_{R_n}^+][X^-]$ , in which  $R$  represents the lengthy hydrocarbon chains either an alkyl or an aryl functional group, and  $X$  either organic or inorganic anion [21]. The chemical structure is depicted in Fig. 1 at the centre of the illustration [21]. The alkyl or aryl functional groups are bonded directly to the nitrogen centre atom, forming a positively charged core nitrogen cation. In comparison to the ammonium ion  $[NH_4^+]$  and the primary,

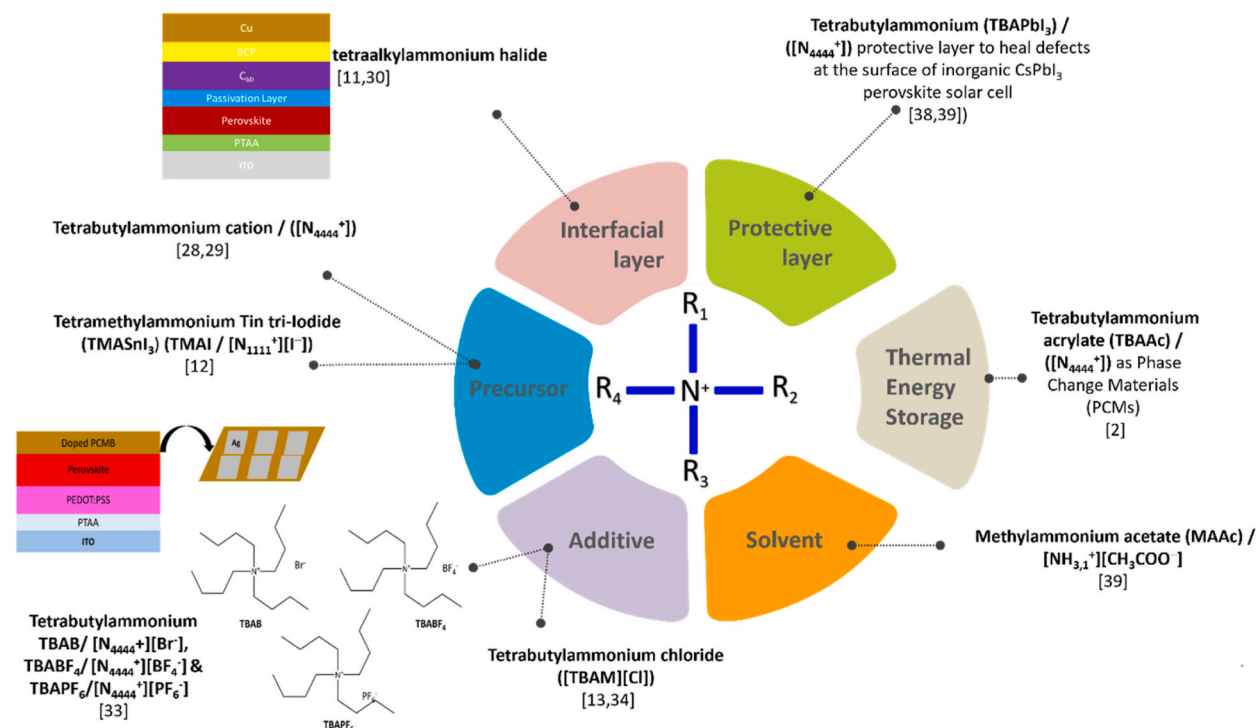


Fig. 1. Tetraalkylammonium salts (TAS) applications in solar energy.

secondary, or tertiary ammonium cations, the quaternary ammonium cations are constantly charged and indicate their pH level in solution [4]. In 1890, Menshutkin developed the compound via nucleophilic replacement of tertiary amines with an alkyl halide, which is known as the “Menschutkin reaction”, and is still considered the best technique for the preparation of quaternary ammonium salts [22]. The basic chemical structure of TAS is composed of two parts, notably a hydrophobic alkyl group and a positively charged hydrophilic core that maintains its cationic feature regardless of the pH level [23]. The physical and chemical properties of TAS are influenced by both of these components [24] as well as its substitutes, especially the alkyl chain [25]. Although common TAS is soluble in water [26], the aqueous solubility of TAS reduces with the increase in hydrophobicity or molecular length of the alkyl chain [27]. Similar to alcohols and water, TAS is extensively soluble in polar and protic solvents due to their ionic charges [13]. As with the aqueous solubility of TAS in water, the solubility of TAS in polar and protic solvents drastically decreases as the chain length increases, while TAS with  $R$  greater than  $C_{14}$  is almost insoluble in water with minimal solubility [28]. Long-chain TAS also exhibits significantly higher solubility in non-polar solvents. Despite that TAS appear as solids, the length and structure of the attached  $R$ -residues can substantially influence their thermal properties [22,29].

## 1.2. TAS applications in solar energy

TAS has been widely used as precursors, additives, solvents, interfacial layers, and protective layers to enhance the power conversion efficiency (PCE), previously in dye-sensitized solar cells (DSSCs) and most recently in PSCs [16–19]. The findings indicate that the roles of TAS demonstrated tangible outcomes, including satisfactory chemical and thermal stability, decent solvent properties, and unique solubility, specifically in solar cell development [29] as illustrated in Fig. 1. Generally, the remarkable enhancement of PSC's PCE, particularly on short-circuit current density ( $J_{sc}$ ), open-circuit voltage ( $V_{oc}$ ), PCE, stability, and low hysteresis is reflected by the degree of crystallinity and structural morphology of perovskite films which could be tune by TAS's structure [30].

### i) TAS as precursor

Precursor are essentially applied to design and synthesize the desired crystallinity and morphological structure. Besides, comprehensive investigations have been carried out to evaluate numerous combinations and permutations of precursor, such as mixing various precursors and introducing different precursors [31]. In a recent study, Bouich et al. [32] explored the impact of incorporating tetrabutylammonium iodide (TBAI/ $[N_{4444}^+][I^-]$ ) as a precursor into the MAPbI<sub>3</sub> solution, forming MA<sub>(1-x)</sub>TBA<sub>x</sub>PbI<sub>3</sub> thin films. This investigation aimed to examine how different percentages of TBAI incorporation affected the structure-property relationship of MAPbI<sub>3</sub>. The findings revealed that introducing TBAI increased crystallinity, and grain size, improved surface morphology without pin-holes, and enhanced roughness in the resulting MAPbI<sub>3</sub> thin films. Furthermore, the MA<sub>(1-x)</sub>TBA<sub>x</sub>PbI<sub>3</sub> thin film exhibited superior stability, particularly in a relative humidity of approximately 60 % after 15 days, compared to the pure MAPbI<sub>3</sub> thin film. Poli et al. [33] also observed an increased hydrophobicity, which produced excellent moisture stability by modifying the perovskite absorbent layer through the addition of tetrabutylammonium iodide (TBAI/ $[N_{4444}^+][I^-]$ ) and methylammonium iodide (MAI/ $[NH_{3,1}^+][I^-]$ ). Since (TBAI/ $[N_{4444}^+][I^-]$ ) is unreactive with water at room temperature, it possesses exceptional thermal and thermodynamic stability, demonstrating the viable application of TAS ions to strengthen the stability of lead halide perovskites [30]. Moreover, Li et al. [34] introduced tetrabutylammonium (TBA) cation ( $[N_{4444}^+]$ ) in mixed-cation lead halide perovskite. TBA cations were then installed at grain boundaries as sacrificial cations to enhance the stability of the respective solar cells. TBA cations are effective materials to enhance solar cell stability in the development of perovskite grains perpendicular to the substrate through heat in contrast to moisture [32].

Due to the inherent instability of perovskite materials in ambient conditions and the environmentally undesirable presence of toxic Pb within perovskite layers, which challenges the principles of green energy technology, Banerjee et al. [18] reported the synthesis of TMA<sub>3</sub>SnI<sub>3</sub> using tetramethylammonium iodide (TMAI/ $[N_{1111}^+][I^-]$ ), which is a lead-free organic-inorganic halide perovskite (OIHP) layer, where the organic TMA cation/ $[N_{1111}^+]$  was employed instead of the standard methylammonium ion  $[NH_{3,1}^+]$ . Based on the results, the photovoltaic response of a basic device structure recorded a PCE of ~1.92%. Hence, the study highlighted the successful synthesis of a lead-free, more environmentally friendly, moisture-resistant PSC, and excellent perovskite material. Meanwhile, Pandey et al. [5] addresses the challenges of lead toxicity in perovskite top cells, proposing a lead-free solution with a maximum conversion efficiency of 30.7 % using MAI/ $[NH_{3,1}^+][I^-]$  in methylammonium tin mixed halide (MASnX<sub>3</sub>) in a tandem solar cell configuration with silicon.

### ii) TAS as solvent

Given the remarkable strides in cost-effectiveness and performance witnessed in solar cell structures, numerous solvents are undergoing development and gradual integration for enhancing the performance of PSC. Hence, Chao et al. [35] proposed the use of methylammonium acetate (MAAc/ $[NH_{3,1}^+][CH_3COO^-]$ ) as an alternative solvent ecologically pleasant normal temperature molten salt for facile synthesis of PSC in the surrounding atmosphere. MAAc/ $[NH_{3,1}^+][CH_3COO^-]$  is non-hazardous and possesses remarkable chemical properties, including impressive viscosity and low vapor pressure. In comprehensive exploration of PSC toward advancing the efficiency and applicability of these photovoltaic devices, Bhattarai et al. [36] focuses on optimizing PSC structures by introducing a double perovskite absorber layer and the use of MAI/ $[NH_{3,1}^+][I^-]$ , showcasing exceptional efficiency of 31.53 % with precise modelling techniques and considering defect density and temperature effects.

### iii) TAS as additive

TAS additives have found extensive application in perovskite precursor solutions with the objective of enhancing the quality of the resulting perovskite film by passivating defects and regulating crystallinity. While there has been thorough exploration into the role of additives in defect passivation, a comprehensive understanding of their influence on the crystallization process of perovskites remains lacking. Yan et al. [37] successfully demonstrated the development of salt-doped films via the integration of 6,6-phenyl-C<sub>61</sub> butyric acid methyl ester (PCBM) with three TAS derivatives containing different counterions, including tetrabutylammonium hexafluorophosphate (TBAPF<sub>6</sub>/[N<sub>4444</sub><sup>+</sup>][PF<sub>6</sub><sup>-</sup>], tetrabutylammonium tetrafluoroborate (TBABF<sub>4</sub>/[N<sub>4444</sub><sup>+</sup>][BF<sub>4</sub><sup>-</sup>]), and tetrabutylammonium bromide (TBABr/[N<sub>4444</sub><sup>+</sup>][Br<sup>-</sup>]), as the electron transport layer (ETL) to enhance the performance of inverted PSC. As opposed to un-doped PCBM films, the developed integrated salt-doped PCBM films recorded greater Fermi levels and electron mobility. The photoluminescence quenching tests, particularly for [N<sub>4444</sub><sup>+</sup>][BF<sub>4</sub><sup>-</sup>], showed an improved charge transfer at the interface between the salt-doped PCBM and perovskite. The electron transporting capabilities of the salt-doped PCBM was also dramatically enhanced, as calculated from the mobility measurements and ultra-violet (UV) photoelectron spectroscopy. Furthermore, the presence of the doping ammonium salts altered and enhanced the surface roughness of the salt-doped PCBM films. Overall, the doping of [N<sub>4444</sub><sup>+</sup>][BF<sub>4</sub><sup>-</sup>] and [N<sub>4444</sub><sup>+</sup>][PF<sub>6</sub><sup>-</sup>] in the PCBM film increased the fill factor and  $J_{sc}$  values, which may be contributed to the use of fluorine-rich salt counterions that improved the device performance.

Another crucial property of TAS is their general characteristic of ILs, which significantly influence the crystallization of perovskite film. Shahiduzzaman et al. [19,38] explored the impact of 3 wt.% TAS at varying viscosity on the development and performance of perovskite crystals by employing a precursor solvent *N,N*-dimethylformamide (DMF). TAS recorded an improved light absorption with smoother film than DMF alone, while tetrabutylammonium chloride TBACl/[N<sub>4444</sub><sup>+</sup>][Cl<sup>-</sup>], was considered the best performing ILs. The dispersion of tiny bunches to assemble and produce nanoparticles was hampered by the increased TAS viscosity, causing the increase in non-homogeneity during the film formation [39]. Moreover, Carrillo et al. [40] demonstrated the potential use of alkyl ammonium cations (MAI/[NH<sub>3,1</sub><sup>+</sup>][I<sup>-</sup>]) to increase moisture tolerance and surface damage by placing a perovskite screen in a methylammonium iodide solution in PSCs.

Very recently, Mohammed et al. [41] delves into hole transport material-free perovskite solar cells, where adding malonic acid as additive to methylammonium lead iodide (MAPbI<sub>3</sub>) significantly enhances stability and efficiency, resulting in a remarkable power conversion efficiency of 14.14 %.

### iv) TAS as interfacial and protective layer

Although perovskite materials exhibit fewer defects compared to other semiconductors, the presence of flaws at the grain boundary or interface could severely affect the effectiveness and stability of the device due to trap-assisted non-radiative recombination [42]. According to Zheng et al. [43], tetraalkylammonium halides may passivate charged defects in OIHP with tetraalkylammonium and halide ions. They employed two different molecular choline zwitterions, also recognized as tetraalkylammonium halides, as the interfacial layer, including choline chloride, [N<sub>1,1,1,2OH</sub><sup>+</sup>][Cl<sup>-</sup>] and choline iodide, [N<sub>1,1,1,2OH</sub><sup>+</sup>][I<sup>-</sup>], which have no significant alkyl chain. In contrast to the approach using PCMB passivation, [N<sub>1,1,1,2OH</sub><sup>+</sup>][Cl<sup>-</sup>] and [N<sub>1,1,1,2OH</sub><sup>+</sup>][I<sup>-</sup>] passivation significantly reduces the trap density. In addition, it extends the carrier lifetime and increases the  $V_{oc}$  of OIHP devices with various bandgaps, which leads to an increase in PCE from 10 % to 35 %. Moreover, the approach improved the stability of the OIHP device with practically zero efficiency loss following 800 h of PCE storage. Hence, the findings reiterated the relevance of the all-around passivation of charged ionic faults to enhance the lifespan and efficiency of OIHP devices [44].

Furthermore, in 2019, Kim et al. [31] conducted a comparative analysis of the PCE and humidity stability of 2D interfacial layers formed perovskite (FAPbI<sub>3</sub>)<sub>0.95</sub>(MAPbBr<sub>3</sub>)<sub>0.05</sub> after treatment with *n*-butylammonium iodide (BAI/[NH<sub>3,4</sub><sup>+</sup>][I<sup>-</sup>]), *n*-octylammonium iodide (OAI/[NH<sub>3,8</sub><sup>+</sup>][I<sup>-</sup>]), and *n*-dodecylammonium iodide (DAI/[NH<sub>3,12</sub><sup>+</sup>][I<sup>-</sup>]), featuring alkylammonium of varying chain lengths. As the alkyl chain length progressed from [NH<sub>3,4</sub><sup>+</sup>] to [NH<sub>3,8</sub><sup>+</sup>] to [NH<sub>3,12</sub><sup>+</sup>], a significant increase in electron blocking and resistance to humidity was observed for [NH<sub>3,4</sub><sup>+</sup>] and [NH<sub>3,8</sub><sup>+</sup>], while the corresponding difference in the case of [NH<sub>3,12</sub><sup>+</sup>] was relatively minor. Notably, the PSC post-treated with [NH<sub>3,8</sub><sup>+</sup>][I<sup>-</sup>] exhibited slightly higher efficiency compared to those with [NH<sub>3,4</sub><sup>+</sup>][I<sup>-</sup>] and [NH<sub>3,8</sub><sup>+</sup>][I<sup>-</sup>], achieving a certified stabilized efficiency of 22.9 %.

Subsequently, TAS are employed as a protective layer. Reducing the dimension of the perovskite layer *in situ* through post-synthesis ion exchange successfully passivated the OIHP. In this treatment, Liu et al. [45] demonstrated the successful intercalation of TBA/[N<sub>4444</sub><sup>+</sup>] cations into CsPbI<sub>3</sub>. This process effectively substituted the Cs cations, forming a one-dimensional TBAPbI<sub>3</sub> layer through post-synthesis TBAl/[N<sub>4444</sub><sup>+</sup>][I<sup>-</sup>] treatment. The introduced TBA/[N<sub>4444</sub><sup>+</sup>] cations facilitated the in-situ creation of a protective TBAPbI<sub>3</sub> layer, addressing surface defects in the inorganic CsPbI<sub>3</sub> perovskite. The TBAPbI<sub>3</sub>/CsPbI<sub>3</sub> perovskite layer exhibited enhanced stability and reduced defect density, and consequently, perovskite solar cell devices achieved improved efficiency.

### v) TAS as electrolyte

In addition, TAS is employed as electrolytes owing to their low toxicity, good surface activity, and high resistance to corrosion and oxidation. In addition to developing essential heirloom applications due to electrolytes in solid supercapacitors and ion batteries owing to anisotropic conduction processes [46], research on TAS-based expansion of ion gels has gained more attraction with a broader electrochemical window [47]. As a substitute, researchers have focused on employing organic iodide as the salt in DSSC to address this constraint. Despite these initial results, Jumaah et al. indicated a PCE of 1.0 %, the compound demonstrated solid-solid transitions

characteristic of ionic liquid crystal behaviour [8]. In addition to the frequently used inorganic salts, including NaI, LiI, and KI, TAS was used as the co-electrolyte in DSSCs. For instance, the combination of TBAI/[N<sub>4444</sub><sup>+</sup>][I<sup>-</sup>] and KI increased the PCE of an artificial DSSC. However, the limited solubility of inorganic salts at ambient temperature presents a fundamental drawback to its use [8,48,49]. The subsequent summary in Fig. 2 presents a chart depicting the efficiency trends in TAS-based solar technology.

### 1.3. Versatility of TAS in several applications

Apart from its prevalent application in the solar energy sector, TAS play a notable role is their potent and broad-spectrum killing effect, extensively utilized in diverse sectors such as in water treatment [50], textile [51], and oil production [52], coatings [53], sterilization of algae [54], safeguarding agricultural products from mould [55], insect and corrosion prevention in wood and building materials [56], sterilization of surgical and medical equipment [57], treating poultry eggs and meat, and cleaning and sterilizing household and food products [58,59]. Furthermore, ionic conductivity is another outstanding property of TAS that makes them excellent electrolytics substances [60]. Their amphiphilic properties allow them to be absorbed in the air-water interface such that the hydrophilic part is in the water and the hydrophobic part is in the air. This arrangement reduces the surface or interfacial tension, making them a unique class of surfactants. TAS possesses a wide range of biological activity, which explains their continuous application as bioactive agents. TAS structure featuring a lengthy alkyl chain segment functioning as a hydrophobic (nonpolar) can infiltrate the nonpolar cell membrane, altering its permeability and leading to cell (bacterial) death. Notably, this vital mechanism exhibits minimal impact on bacterial resistance and susceptibility. In fact, TAS is usually identified as a bioactive substance, as has been demonstrated for water-soluble alkyl chains ranging in length from C<sub>8</sub> to C<sub>16</sub> [22]. The distinctive structure of TAS gives them various physical and chemical capabilities, including emulsification, dispersion, solubilization, and sterilization [52]. TAS has also found widespread use in the field of antibacterial [16,61–63]. Overall, the unique physicochemical properties of TAS make them a preferable component in various applications and industrial production [64].

## 2. Potential toxicity impact of TAS

The toxicity of TAS has eventually drawn the attention of researchers, especially those in the field of renewable energy and green chemistry. Interestingly, the non-volatile properties of TAS, which contribute to their potential renewable alternatives in place of traditional volatile organic solvents, are the primary justification for their status as non-toxic substances [65]. Unfortunately, this assumption is misleading and has triggered disputes over the toxicity level of TAS. While TAS have been shown to facilitate air pollution mitigation, the unregulated discharge of TAS into aquatic ecosystems could cause severe water contamination due to their possible toxic level and poor biodegradability [66]. Globally, the concentration of TAS in wastewater was detected at a range of 1–60 µg/L and is predicted to multiply 10 times in influential wastewater [67]. Hence, investigation of the toxicity of TAS through various approaches, such as the cytotoxicity test, has progressed rapidly with in-depth insights and new understanding despite a recent decline in the toxicity level of TAS.

New generation TAS have been identified as part of the grand strategy to design and synthesize bio-renewable degradable and ILs. The expansion of the TAS-based field is supported by the publication of numerous excellent articles that covered different topics concerning ILs. Thus, the present review explores the recent developments of toxicological TAS upon exposure to humans,

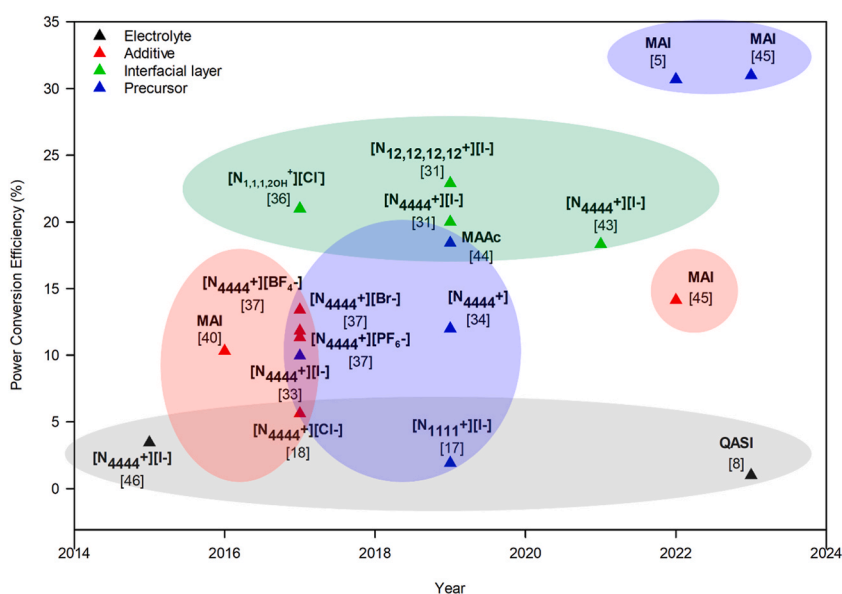
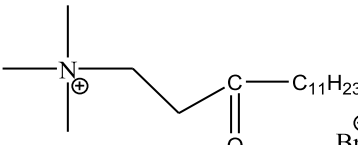
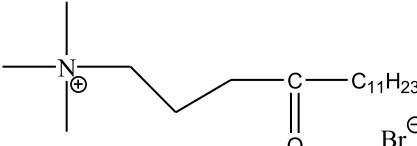
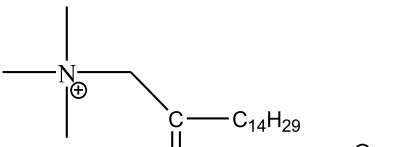
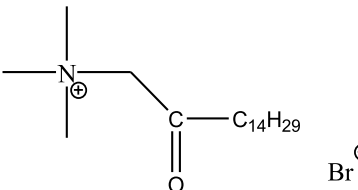
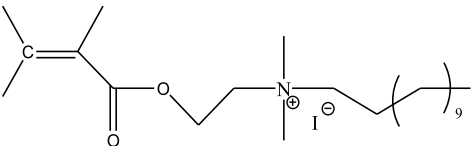


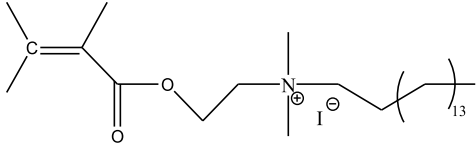
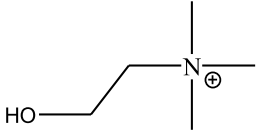
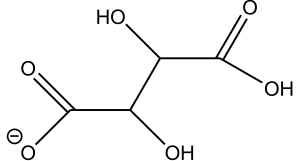
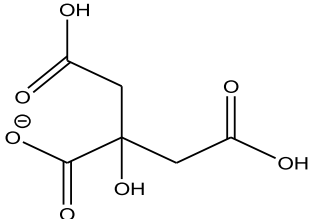
Fig. 2. The summary of the TAS based solar cell efficiency.

**Table 1**  
*In Vitro* cytotoxicity of TAS.

TAS	Strain/Sel/Organism	MIC, CC/IC/EC/LC/ED/LD <sub>50</sub>	References
<p><b>MTT Assays</b></p> <p>2-dodecanoyloxyethyl)trimethylammonium bromide (DMM-11) [N<sub>1,1,1,CH<sub>2</sub>C(O)C<sub>11</sub>H<sub>23</sub>][Br<sup>-</sup>]</sub></p> 	A375 -Melanoma cells HT-29- Colon adenocarcinoma cells NHDFs cell- Normal human dermal fibroblast cells	IC <sub>50</sub> = 0.01875 mg/L IC <sub>50</sub> = 0.0125 mg/L IC <sub>50</sub> = 0.350 mg/L	[71]
<p>2-dodecanoyloxypropyl)trimethylammonium bromide (DMPM-11) [N<sub>1,1,1,C<sub>3</sub>C(O)C<sub>11</sub>H<sub>23</sub>][Br<sup>-</sup>]</sub></p> 	A375 -Melanoma cells HT-29- Colon adenocarcinoma cells NHDFs cell- Normal human dermal fibroblast cells	IC <sub>50</sub> = 0.0156 mg/L IC <sub>50</sub> = 0.09 mg/L IC <sub>50</sub> = 0.6 mg/L	[71]
<p>2-pentadecanoyloxymethyl)trimethylammonium bromide (DMGM-14) [N<sub>1,1,1,CC(O)C<sub>14</sub>H<sub>29</sub>][Br<sup>-</sup>]</sub></p> 	A375 -Melanoma cells HT-29- Colon adenocarcinoma cells NHDFs cell- Normal human dermal fibroblast cells	IC <sub>50</sub> = 0.00195 mg/L IC <sub>50</sub> = 0.0156 mg/L IC <sub>50</sub> = 0.2375 mg/L	[71]
<p>2-dimethyl-2-dodecyl-1-methacryloxyethyl ammonium iodine (DDMAI) [N<sub>1,1,1,1,CC(O)C=C<sup>+</sup>][I<sup>-</sup>]</sub></p> 	L929 mouse fibroblast cells	Concentrations up to 20 μg/ml	[72]
<p>Dimethyl-hexadecyl-methacryloxyethyl-ammonium iodide (DHMAI) [N<sub>1,1,1,1,6,C<sub>20</sub>C(O)C=C<sup>+</sup>][I<sup>-</sup>]</sub></p> 	L929 mouse fibroblast cells	Concentrations up to 5 μg/ml	[72]

(continued on next page)

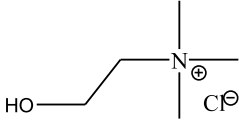
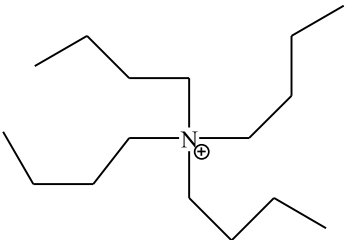
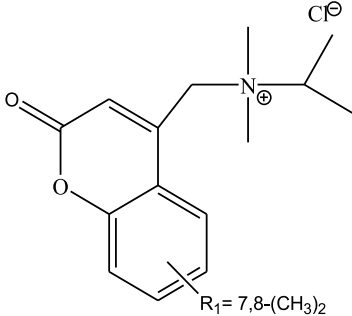
Table 1 (continued)

TAS	Strain/Sel/Organism	MIC, CC/IC/EC/LC/ED/LD <sub>50</sub>	References
 <p>Choline-based ionic liquids [N<sub>1,1,1,2OH</sub><sup>+</sup>]</p>	MCF-7 cells -Human breast cancer cell line	IC <sub>50</sub> [N <sub>1,1,1,2OH</sub> <sup>+</sup> ][Cl <sup>-</sup> ] = 522.0 mM IC <sub>50</sub> [N <sub>1,1,1,2OH</sub> <sup>+</sup> ][Br <sup>-</sup> ] = 127.0 mM IC <sub>50</sub> [N <sub>1,1,1,2OH</sub> <sup>+</sup> ][I <sup>-</sup> ] = 94.66 mM IC <sub>50</sub> [N <sub>1,1,1,2OH</sub> <sup>+</sup> ][Bit <sup>-</sup> ] = 53.60 mM IC <sub>50</sub> [N <sub>1,1,1,2OH</sub> <sup>+</sup> ][Dhc <sup>-</sup> ] = 15.92 mM	[73]
 <p>[N<sub>1,1,1,2OH</sub><sup>+</sup>][Cl<sup>-</sup>]            [N<sub>1,1,1,2OH</sub><sup>+</sup>][Br<sup>-</sup>]            [N<sub>1,1,1,2OH</sub><sup>+</sup>][I<sup>-</sup>]            [N<sub>1,1,1,2OH</sub><sup>+</sup>][Bit<sup>-</sup>]</p>			
 <p>[N<sub>1,1,1,2OH</sub><sup>+</sup>][Dhc<sup>-</sup>]</p>			
 <p>Choline-based ionic liquids [N<sub>1,1,1,2OH</sub><sup>+</sup>]</p>	HEK-293- human embryonic kidney cells	IC <sub>50</sub> = 62.88 mM	[74]

7

(continued on next page)

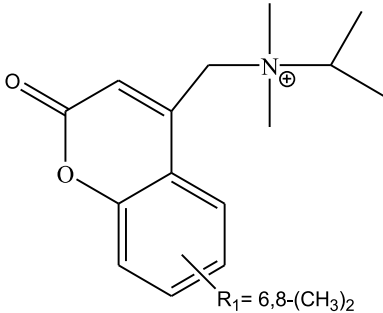
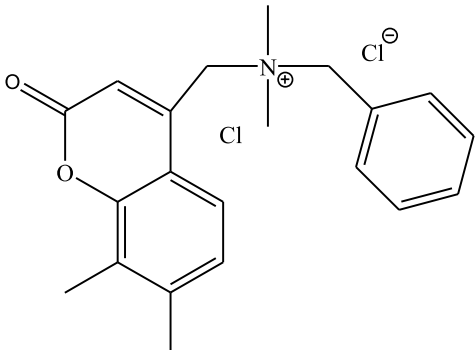
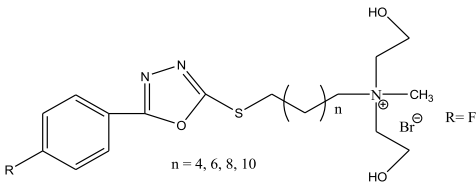
Table 1 (continued)

TAS	Strain/Sel/Organism	MIC, CC/IC/EC/LC/ED/LD <sub>50</sub>	References
 <p>[N<sub>1,1,1,2OH</sub>]<sup>+</sup>[Cl<sup>-</sup>] Tetrabutylammonium based ionic liquid (TBA/[N<sub>4444</sub>])</p>	Human-derived colon carcinoma cells (Caco-2)	IC <sub>50</sub> = 309.4 mg/L	[75]
 <p>Tetraalkylammonium chlorides (i)</p>	Human liver cancer (HepG2) Human colorectal cancer (Caco-2) Mouse fibroblast (L-929) cell lines	IC <sub>50</sub> = 130.5 ± 22.6 μm IC <sub>50</sub> = 212.6 ± 14.1 μM IC <sub>50</sub> = 223.9 ± 11.6 μM	[76]
 <p>R<sub>1</sub> = 7,8-(CH<sub>3</sub>)<sub>2</sub></p>			

(continued on next page)

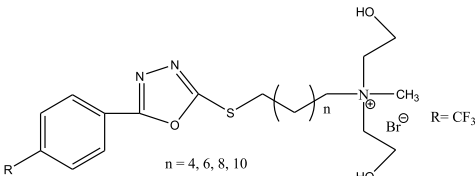
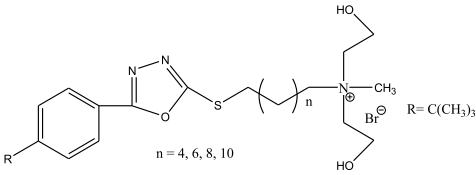
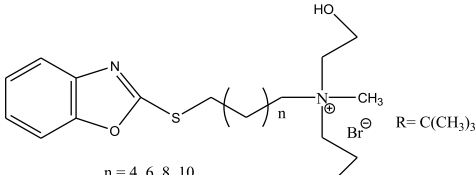
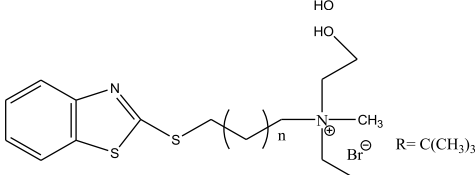
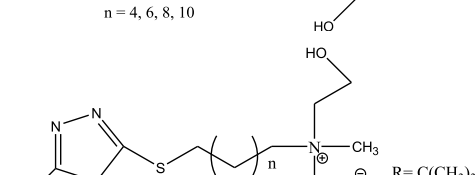


Table 1 (continued)

TAS	Strain/Sel/Organism	MIC, CC/IC/EC/LC/ED/LD <sub>50</sub>	References
<p>Tetraalkylammonium chlorides (ii)</p>  <p>R<sub>1</sub> = 6,8-(CH<sub>3</sub>)<sub>2</sub></p>	<p>Human liver cancer (HepG2) Human colorectal cancer (Caco-2) Mouse fibroblast (L-929) cell lines</p>	<p>IC<sub>50</sub> = 202.3 ± 16.2 μM IC<sub>50</sub> = 108.6 ± 1.9 μM IC<sub>50</sub> = &gt;350 μM</p>	[76]
<p>Tetraalkylammonium chlorides (iii)</p> 	<p>Human liver cancer (HepG2) Human colorectal cancer (Caco-2) Mouse fibroblast (L-929) cell lines</p>	<p>IC<sub>50</sub> = 225.6 ± 15.2 μM IC<sub>50</sub> = 147.4 ± 14.8 μM IC<sub>50</sub> = &gt;350 μM</p>	[76]
<p>Six sets of novel TASs were prepared for analysis by changing or substituting the 5-phenyl-1,3,4-oxadiazole-2-thiol (POT) fragments in C<sub>12</sub>TAS</p>  <p>n = 4, 6, 8, 10</p> <p>R = F</p>	<p>Human immortalised epidermal (HaCaT) Human normal liver (LO2) cell line</p>	<p>IC<sub>50</sub> = 6.14 ~ 76.52 μg/mL IC<sub>50</sub> = 6.95 ~ 83.51 μg/mL</p>	[77]

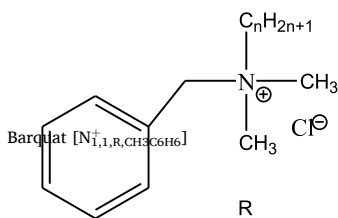
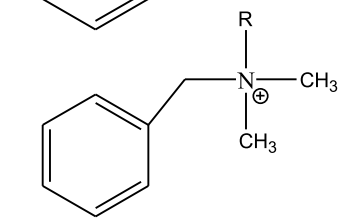
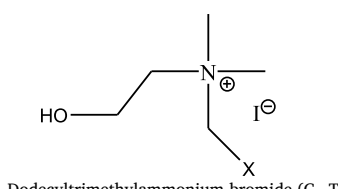
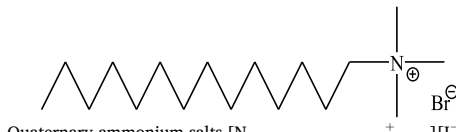
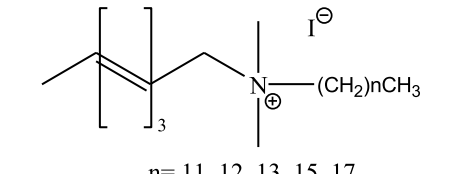
(continued on next page)

Table 1 (continued)

TAS	Strain/Sel/Organism	MIC, CC/IC/EC/LC/ED/LD <sub>50</sub>	References
 <p>n = 4, 6, 8, 10 R = CF<sub>3</sub></p>	Human immortalised epidermal (HaCaT) Human normal liver (LO2) cell line	IC <sub>50</sub> = 5.25 ~ 62.57 μg/mL IC <sub>50</sub> = 5.86 ~ 74.35 μg/mL	[77]
 <p>n = 4, 6, 8, 10 R = C(CH<sub>3</sub>)<sub>3</sub></p>	Human immortalised epidermal (HaCaT) Human normal liver (LO2) cell line	IC <sub>50</sub> = 4.16 ~ 23.84 μg/mL IC <sub>50</sub> = 5.08 ~ 44.26 μg/mL	[77]
 <p>n = 4, 6, 8, 10 R = C(CH<sub>3</sub>)<sub>3</sub></p>	Human immortalised epidermal (HaCaT) Human normal liver (LO2) cell line	IC <sub>50</sub> = 7.14 ~ 54.62 μg/mL IC <sub>50</sub> = 9.96 ~ 88.27 μg/mL	[77]
 <p>n = 4, 6, 8, 10 R = C(CH<sub>3</sub>)<sub>3</sub></p>	Human immortalised epidermal (HaCaT) Human normal liver (LO2) cell line	IC <sub>50</sub> = 6.02 ~ 45.06 μg/mL IC <sub>50</sub> = 8.96 ~ 64.28 μg/mL	[77]
 <p>n = 4, 6, 8, 10 R = C(CH<sub>3</sub>)<sub>3</sub></p>	Human immortalised epidermal (HaCaT) Human normal liver (LO2) cell line	IC <sub>50</sub> = 30.12 ~ >100 μg/mL IC <sub>50</sub> = 27.03 ~ >100 μg/mL	[77]
Benzalkonium chloride [N <sub>1</sub> <sup>+</sup> , <sub>1</sub> C <sub>n</sub> H <sub>2n+1</sub> CH <sub>3</sub> C <sub>6</sub> H <sub>6</sub> ][Cl <sup>-</sup> ]	Zebrafish liver cells (ZFL) Human hepatoma cell line (Huh7)	EC <sub>50</sub> = 1.82 μg/mL EC <sub>50</sub> = 4.23 μg/mL	[78]

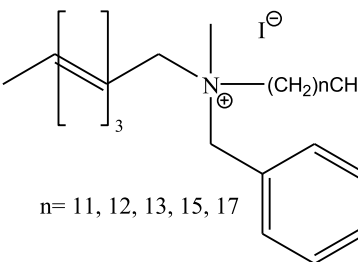
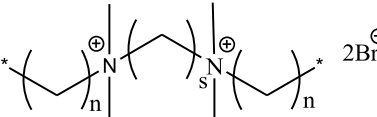
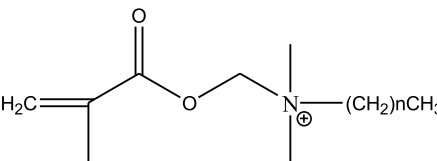
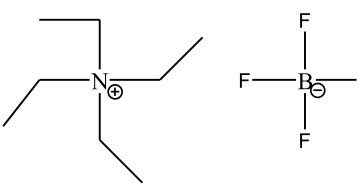
(continued on next page)

Table 1 (continued)

TAS	Strain/Sel/Organism	MIC, CC/IC/EC/LC/ED/LD <sub>50</sub>	References
 <p>Barquat [N<sub>1,1,R,CH<sub>3</sub></sub>C<sub>6</sub>H<sub>6</sub>]<sup>+</sup> Cl<sup>-</sup></p>	Zebrafish liver cells (ZFL) Human hepatoma cell line (Huh7)	EC <sub>50</sub> = 1.19 μg/mL EC <sub>50</sub> = 3.4 μg/mL	[78]
 <p>Halomethylated quaternary ammonium salts (series I) [N<sub>1,1,CH<sub>3</sub>,C<sub>3</sub>OH</sub>]<sup>+</sup> [I<sup>-</sup>]</p>	Human promonocytic cells U-937	LC <sub>50</sub> = 21–45 μg/mL iodinated salts, LC <sub>50</sub> = 9–46 μg/mL	[79]
 <p>Dodecyltrimethylammonium bromide (C<sub>12</sub>TAB/[N<sub>1,1,1,1,2</sub>]<sup>+</sup> [Br<sup>-</sup>])</p>	Human intestinal columnar epithelial cell line C2BBE1 (ATCC)	IC <sub>50</sub> = (C <sub>12</sub> TAB) 6.2–8.2 μM	[80]
 <p>Quaternary ammonium salts [N<sub>1,1,(CH<sub>2</sub>)<sub>n</sub>CH<sub>3</sub>,CH<sub>3</sub>(C=C)<sub>3</sub>CH<sub>3</sub>]<sup>+</sup> [I<sup>-</sup>]</sub></p>	The long-term human microvascular endothelial cell line (HMEC)	IC <sub>50</sub> = 5.63 ~ >20 μM	[81]
 <p>n = 11, 12, 13, 15, 17</p>			

(continued on next page)

Table 1 (continued)

TAS	Strain/Sel/Organism	MIC, CC/IC/EC/LC/ED/LD <sub>50</sub>	References
Quaternary ammonium salts $[N_1, (CH_2)_nCH_3, CH_3C_6H_6, CH_3(C=\overset{\oplus}{C})_3CH_3][I^-]$  n= 11, 12, 13, 15, 17	The long-term human microvascular endothelial cell line (HMEC)	IC <sub>50</sub> = 5.90–22.99 μM	[81]
Gemini quaternary ammonium surfactants  $2Br^\ominus$	<i>C6 glioma</i> HEK293 human kidney cell lines	IC <sub>50</sub> = 2.2–12.0 μg/ml IC <sub>50</sub> = 2.2–5.0 μg/ml	[82]
2-dimethylamino ethyl methacrylate (DMAEMA), $[N_{1,1}, (CH_2)_nCH_3, CH_3OC(O)CH_2-\overset{\oplus}{C}CH_3]$ 	Human gingival fibroblasts (HGF) Odontoblast-like MDPC-23 mice cells	At concentration of 0.5 μg/ml, cell viability was still excellent for DMAEMA	[83]
Other Assays Tetraethylammonium tetrafluoroborate (TEABF <sub>4</sub> /[N <sub>2222</sub> ][BF <sub>4</sub> <sup>-</sup> ])	PrestoBlue Cell Viability on seven human cell lines:- (i) HEK293 (human embryonic kidney) (ii) U937 (human myeloid leukemia) (iii) Jurkat (human T-cell leukemia) (iv) HL60 (human acute promyelocytic leukemia) (v) K562 (human chronic myelogenous leukemia) (vi) A549 (human alveolar adenocarcinoma) (vii) A2780 (human ovarian carcinoma)	CC <sub>50</sub> (HEK293) = 42.050 mM CC <sub>50</sub> (U937) = 13.160 mM CC <sub>50</sub> (Jurkat) = 11.080 mM CC <sub>50</sub> (HL60) = 10.210 mM CC <sub>50</sub> (K562) = 14.260 mM CC <sub>50</sub> (A549) = 27.070 mM CC <sub>50</sub> (A2780) = 29.440 mM	[84]
Tetrabutylammonium chloride (TBACl/[N <sub>4444</sub> ][Cl <sup>-</sup> ]) 	PrestoBlue Cell Viability on seven human cell lines:-	CC <sub>50</sub> (HEK293) = 25.340 mM CC <sub>50</sub> (U937) = 8.990 mM	[84]

(continued on next page)

Table 1 (continued)

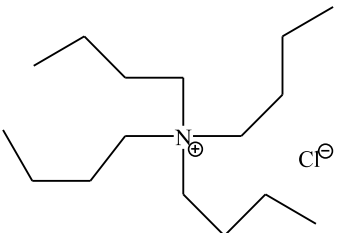
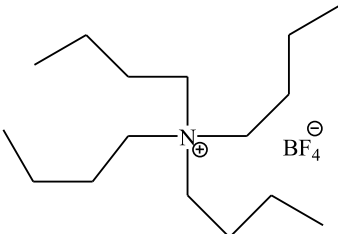
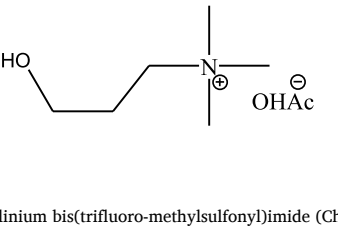
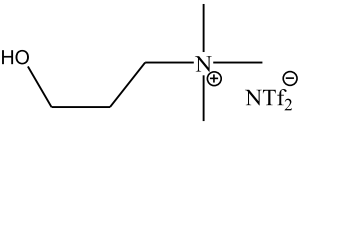
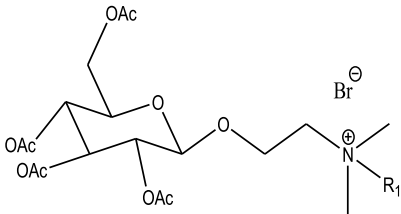
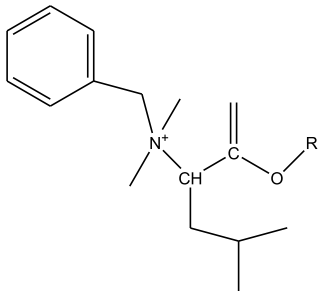
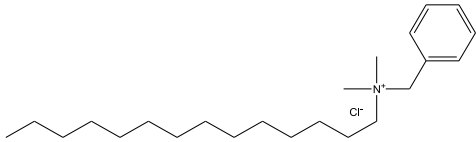
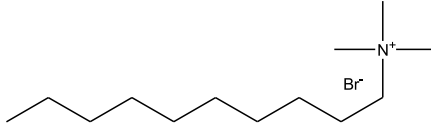
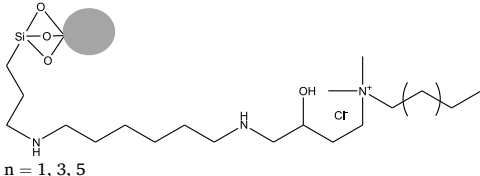
TAS	Strain/Sel/Organism	MIC, CC <sub>50</sub> /IC <sub>50</sub> /EC <sub>50</sub> /LC <sub>50</sub> /ED <sub>50</sub> /LD <sub>50</sub>	References
 <p>Tetrabutylammonium tetrafluoroborate (TBABF<sub>4</sub>/[N<sup>+</sup><sub>4444</sub>][BF<sub>4</sub><sup>-</sup>])</p>	(ii) U937 (human myeloid leukemia) (iii) Jurkat (human T-cell leukemia) (iv) HL60 (human acute promyelocytic leukemia) (v) K562 (human chronic myelogenous leukemia) (vi) A549 (human alveolar adenocarcinoma) (vii) A2780 (human ovarian carcinoma)	CC <sub>50</sub> (Jurkat) = 5.390 mM CC <sub>50</sub> (HL60) = 1.790 mM CC <sub>50</sub> (K562) = 12.590 mM CC <sub>50</sub> (A549) = 25.340 mM CC <sub>50</sub> (A2780) = 12.970 mM	
 <p>Cholinium acetate (CholOAc/[N<sup>+</sup><sub>1,1,1,2OH</sub>][CH<sub>3</sub>COO<sup>-</sup>])</p>	PrestoBlue Cell Viability on seven human cell lines:- (i) HEK293 (human embryonic kidney) (ii) U937 (human myeloid leukemia) (iii) Jurkat (human T-cell leukemia) (iv) HL60 (human acute promyelocytic leukemia) (v) K562 (human chronic myelogenous leukemia) (vi) A549 (human alveolar adenocarcinoma) (vii) A2780 (human ovarian carcinoma)	CC <sub>50</sub> (HEK293) = 27.520 mM CC <sub>50</sub> (U937) = 8.540 mM CC <sub>50</sub> (Jurkat) = 4.960 mM CC <sub>50</sub> (HL60) = 2.230 mM CC <sub>50</sub> (K562) = 8.370 mM CC <sub>50</sub> (A549) = 16.760 mM CC <sub>50</sub> (A2780) = 11.650 mM	[84]
 <p>Cholinium bis(trifluoro-methylsulfonyl)imide (Chol NTf<sub>2</sub>/[N<sup>+</sup><sub>1,1,1,2OH</sub>][NTf<sub>2</sub><sup>-</sup>])</p>	PrestoBlue Cell Viability on seven human cell lines:- (i) HEK293 (human embryonic kidney) (ii) U937 (human myeloid leukemia) (iii) Jurkat (human T-cell leukemia) (iv) HL60 (human acute promyelocytic leukemia) (v) K562 (human chronic myelogenous leukemia) (vi) A549 (human alveolar adenocarcinoma) (vii) A2780 (human ovarian carcinoma)	CC <sub>50</sub> (HEK293) = 256.150 mM CC <sub>50</sub> (U937) = 137.770 mM CC <sub>50</sub> (Jurkat) = 153.090 mM CC <sub>50</sub> (HL60) = 100.400 mM CC <sub>50</sub> (K562) = 86.620 mM CC <sub>50</sub> (A549) = 143.140 mM CC <sub>50</sub> (A2780) = 149.100 mM	[84]
	PrestoBlue Cell Viability on seven human cell lines:- (i) HEK293 (human embryonic kidney) (ii) U937 (human myeloid leukemia) (iii) Jurkat (human T-cell leukemia) (iv) HL60 (human acute promyelocytic leukemia) (v) K562 (human chronic myelogenous leukemia) (vi) A549 (human alveolar adenocarcinoma) (vii) A2780 (human ovarian carcinoma)	CC <sub>50</sub> (HEK293) = 24.330 mM CC <sub>50</sub> (U937) = 7.240 mM CC <sub>50</sub> (Jurkat) = 5.120 mM CC <sub>50</sub> (HL60) = 3.120 mM CC <sub>50</sub> (K562) = 7.280 mM CC <sub>50</sub> (A549) = 13.400 mM CC <sub>50</sub> (A2780) = 15.150 mM	[84]

Table 1 (continued)

TAS	Strain/Sel/Organism	MIC, CC/IC/EC/LC/ED/LD <sub>50</sub>	References
Quaternary Ammonium Bromides Using D-Glucose as a Substrate [ $N_{1,1,1,2OH}^+$ ][ $NTf_2^-$ ]	WST-1 test on IPC-81 Rat Leukemia Cell Line	EC <sub>50</sub> = 9.5–85.1 $\mu$ mol	[85]
 <p>Benzyl quaternary ammonium leucine-based surfactants</p>	<p>MTS assays:-</p> <p>i) Intestinal epithelial (Caco-2)</p> <p>ii) Airway epithelial (Calu-3)</p>	<p>C<sub>10</sub></p> <p>i) EC<sub>50</sub> (Caco-2) = 0.160 <math>\pm</math> 0.007 mM</p> <p>ii) EC<sub>50</sub> (Calu-3) = 0.117 <math>\pm</math> 0.005 mM</p> <p>C<sub>12</sub></p> <p>i) EC<sub>50</sub> (Caco-2) = 0.016 <math>\pm</math> 0.003 mM</p> <p>ii) EC<sub>50</sub> (Calu-3) = 0.011 <math>\pm</math> 0.002 mM</p> <p>C<sub>14</sub></p> <p>i) EC<sub>50</sub> (Caco-2) = 0.013 <math>\pm</math> 0.002 mM</p> <p>ii) EC<sub>50</sub> (Calu-3) = 0.014 <math>\pm</math> 0.002 mM</p>	[69]
 <p>Benzyl quaternary ammonium leucine-based surfactants</p>	<p>LDH assays:-</p> <p>i) Intestinal epithelial (Caco-2)</p> <p>ii) Airway epithelial (Calu-3)</p>	<p>C<sub>10</sub></p> <p>i) EC<sub>50</sub> (Caco-2) = 0.158 <math>\pm</math> 0.015 mM</p> <p>ii) EC<sub>50</sub> (Calu-3) = 0.187 <math>\pm</math> 0.024 mM</p> <p>C<sub>12</sub></p> <p>i) EC<sub>50</sub> (Caco-2) = 0.019 <math>\pm</math> 0.002 mM</p> <p>ii) EC<sub>50</sub> (Calu-3) = 0.019 <math>\pm</math> 0.003 mM</p> <p>C<sub>14</sub></p> <p>i) EC<sub>50</sub> (Caco-2) = 0.012 <math>\pm</math> 0.002 mM</p> <p>ii) EC<sub>50</sub> (Calu-3) = 0.014 <math>\pm</math> 0.002 mM</p>	[69]

(continued on next page)

Table 1 (continued)

TAS	Strain/Sel/Organism	MIC, CC/IC/EC/LC/ED/LD <sub>50</sub>	References
<p>Benzyltrimethyltetradecylammonium chloride (BAC)</p> 	<p>MTS assays:-</p> <p>i) Intestinal epithelial (Caco-2)</p> <p>ii) Airway epithelial (Calu-3)</p> <p>LDH assays:-</p> <p>i) Intestinal epithelial (Caco-2)</p> <p>ii) Airway epithelial (Calu-3)</p>	<p>MTS assay</p> <p>i) EC<sub>50</sub> (Caco-2) = 0.033 ± 0.001 mM</p> <p>ii) EC<sub>50</sub> (Calu-3) = 0.022 ± 0.005 mM</p> <p>LDH assay</p> <p>i) EC<sub>50</sub> (Caco-2) = 0.048 ± 0.004 mM</p> <p>ii) EC<sub>50</sub> (Calu-3) = 0.029 ± 0.005 mM</p>	[69]
<p>Decyltrimethylammonium bromide (C<sub>10</sub>TAB)</p> 	<p>LDH cytotoxicity assay on MDCK II cells</p>	<p>LD<sub>50</sub> = 3.1 mM</p>	[69,86]
<p>Quaternary ammonium (QA) epoxides/[N<sub>1,1</sub>(CH<sub>2</sub>)<sub>n</sub>, AHAP TMOs][I<sup>-</sup>]</p>  <p>n = 1, 3, 5</p>	<p>MTS assays on L929 mouse fibroblasts</p>	<p>Cytotoxicity = 4.0 µg/mL</p>	[87]

microorganisms, and animals. While TAS remains to be associated with “green” properties, a growing opposing viewpoint among researchers has emerged following a more comprehensive evaluation of the life cycle of TAS. A significant number of research studies have pointed out the toxic impact of ILs on different specimens, including the effect on cells (death rate, morphology, apoptosis, and viability), the toxicity on animals, and the rate of seed germination. The overall toxicity impact of TAS on the environment and human health can be assessed by obtaining toxicity data from different species and cell lines as well as describing its toxicity function [68]. This would establish the foundation for the development of a new TAS that is fully non-toxic, environmentally friendly, and meets all the stipulated requirements.

Most of the past studies assessed the physicochemical properties of TAS, which include decomposition temperature, ionic conductivity, viscosity, solubility, water, density, melting point, and surface tension. As a result, TAS has become a preferred material for various industrial purposes, especially as electrolytes in solar cell applications [8,69]. However, the lack of toxicity information on TAS on the environmental implications limits its optimal use. Cytotoxicity refers to the toxic property of a substance toward living cells. The risk assessment via the screening of mammalian cell cultures is a ground-breaking method in environmental research. Basically, the cytotoxicity test of TAS can be performed in two ways, namely *in vitro* and *in vivo* method. The former method is based on precise cellular mechanisms to detect specific chemicals, while the latter assesses the influence of toxic integration on the whole organism and presents direct effects on environmental specimens. Accordingly, cytotoxicity assays using cell lines have been proven to be excellent indicators of the level of chemical toxicity. Regardless, cytotoxicity assays are comparatively simple, cheaper, and provide rapid results compared to the more costly and time-consuming conventional animal testing methods. Hence, the opportunity to explore the toxicity effects of TAS based on the hydrophilic and hydrophobic properties, which have yet to be studied to date, would provide valuable insights into toxicity information and hazard assessment of TAS. Several *in vitro* and *in vivo* studies on the effect of TAS toxicity on various biological models, particularly cell lines, aquatic models, microorganisms, and mammals, have provided extensive data sets and depict certain relationship trends between the TAS structure and organism activity. Thus, the following sections present a comprehensive overview of the available TAS and the *in vitro* and *in vivo* cytotoxicity analysis in living organisms. As a result, a substance's cytotoxic potential is often utilized as an early toxicity signal. The following discussion summarizes the available cytotoxicity test with several notable examples of TAS-related tests.

### 2.1. *In vitro* cytotoxicity

The study of *in vitro* cytotoxicity plays a pivotal role in unravelling the safety and biocompatibility of chemical compounds, particularly in the realm of potential applications in various fields, including solar applications and materials science. To assess the resulting cell death effectively, there is a need for cost-effective, dependable, and easily reproducible short-term assays for cytotoxicity and cell viability. The (3-(4,5-dimethylthiazol-2-yl)-2,5-diphenyltetrazolium bromide) (MTT) assay is the most common test to evaluate the effect of TAS cytotoxicity on cell viability [70]. Generally, cell viability is measured by verifying the effect of mitochondrial enzymes on the cells [71]. Subsequently, nicotinamide adenine dinucleotide phosphate (NADH) dependent cellular oxidoreductase enzymes induce the MTT to form purple formazan in which the intensity of the substance can be measured through light absorbance at a given wavelength. The procedure is improved given its simplicity, reliability, highly reproducible, and frequently used to examine both the cytotoxicity level and cell viability. The present *in vitro* cytotoxicity of TAS using MTT assays also summarized in Table 1.

In the present study, Hyla et al. [72] investigated the impact of three TAS surfactants—namely, dodecanoyloxypropyl)trimethylammonium bromide (DMPM-11), 2-dodecanoyloxyethyl)trimethylammonium bromide (DMM-11), and 2-pentadecanoyloxymethyl)trimethylammonium bromide (DMGM-14) on specific cell lines, including melanoma A375, colon adenocarcinoma HT-29, and normal human dermal fibroblast (NHDF) cells. The evaluation was carried out selectively using the MTT assay. The study presents IC<sub>50</sub> values for DMPM-11 were 0.00195 mg/ml (A375), 0.09 mg/ml (HT-29) and 0.6 mg/ml (NHDFs). The obtained IC<sub>50</sub> doses for the DMM-11 were 0.01875 mg/ml (A375), 0.09 mg/ml (HT-29), 0.350 mg/ml and for the DMGM-14, 0.4375 mg/ml (A375), 0.0156 mg/ml (HT-29) and 0.2375 mg/ml. The findings reveal that these compounds exhibit significantly lower toxicity towards NHDF cells compared to A375 and HT-29 cancer cells. Importantly, the liposomes containing these compounds demonstrated reduced cytotoxicity in normal cell lines compared to cancer cell lines, presenting encouraging possibilities for their potential use in therapeutic applications. The utilization of nano-formulations offers a promising avenue to enhance the delivery of TAS surfactants, potentially improving their efficacy in anticancer therapy. In addition, Rao et al. [73] assessed the cytotoxicity of synthesized TAS-based monomers, dimethyl-hexadecyl-methacry-loxyethyl-ammonium iodide (DHMAI) and 2-dimethyl-2-dodecyl-1-methacry-loxyethyl ammonium iodine (DDMAI) on L929 mouse fibroblast cells. The results indicate that DHMAI at concentrations up to 5 µg/mL and DDMAI at concentrations up to 20 µg/mL show significantly less toxicity, suggesting that DHMAI and DDMAI monomers are biocompatible at lower concentrations. However, the cytotoxicity of these monomers appears to increase with higher doses, suggesting that using elevated concentrations may reduce cell viability.

Recently, the synthesis of TAS from natural sources, such as choline, has attracted the interest of scientific and industrial players due to their long-term exquisiteness and potentially minimal toxic level. These features unveil new possibilities in other field applications, highlighting the importance to understand the toxicity of these substances. As such, Wang et al. [74] explored the cytotoxicity of five choline [N<sub>1,1,1,2OH</sub><sup>+</sup>]-based TAS on MCF-7 cells (human breast cancer cell line) to assess the alternative utilization of natural and bio-based compounds to replace their conventional counterparts and achieve novel, safe, and functional TAS. The findings indicate that among the five choline [N<sub>1,1,1,2OH</sub><sup>+</sup>]-based TAS, [N<sub>1,1,1,2OH</sub><sup>+</sup>][Cl<sup>-</sup>] exhibits the lowest toxicity, whereas [N<sub>1,1,1,2OH</sub><sup>+</sup>][Dhc<sup>-</sup>] demonstrates the highest toxicity. Furthermore, the results highlight that [N<sub>1,1,1,2OH</sub><sup>+</sup>][Bit<sup>-</sup>] and [N<sub>1,1,1,2OH</sub><sup>+</sup>][Dhc<sup>-</sup>] display elevated toxicity due to the acidity of their solutions, falling below the optimal pH range. Such acidic conditions can potentially impact the



structure of proteins on the cell membrane, leading to cell dysfunction, and in severe cases, causing disruption to the cell membrane and cell wall. Ahmadi et al. [76] also assessed the cytotoxicity of choline-based TAS against human HEK-293 cells and revealed a quadratic relationship between the number of carbon atoms and cytotoxicity level. The hydrophobicity and size of compounds can be correlated with the number of carbon atoms. The result suggests that both large and small number of carbon atom compounds exhibited the least cytotoxicity, while those of average hydrophobicity recorded the highest cytotoxicity.

Meanwhile, Karatas et al. [77] synthesized three tetraalkylammonium chlorides ((i), (ii) and (iii)) given the limited data on the synthesis and toxicity evaluation of ionic or TAS derivatives). Subsequently, cytotoxic characteristics of the three substances were evaluated on colorectal (Caco-2) and human liver (HepG2) cancer cell lines as well as non-cancer mice fibroblasts (L-929). Comparatively, the  $IC_{50}$  value of compound (i) indicates higher toxicity against HepG2 cells and L-929 cells than those of compounds (ii) and (iii). Conversely, compounds (ii) and (iii) exhibited greater toxicity against Caco-2 cells than (i). Apart from cancer cell lines, epithelial cells have often been selected to study cytotoxicity since it is the most immediate layer exposed to harmful elements. Xie et al. [78] studied the toxicity of TAS on human immortalised epidermal (HaCaT) and human normal liver cells (LO2), which represent the human epithelial cells. It was observed that all six novel TAS compounds were non-toxic against LO2 and HaCaT. In fact, their cytotoxicity improved synchronously following the increased chain length from hexyl to dodecyl. The inclusion of long-chain structures and two flexible hydroxyethyl groups in TAS facilitates their efficient penetration through the cell membrane. This enables them to effectively interact with enzymes, thereby passivating them. Additionally, the introduction of the POT fragment in TAS proves to be effective in reducing cytotoxicity.

As mentioned earlier, the uncontrolled utilization of TAS has led to the frequent contamination of natural water bodies and aquatic environments. Although they may exist in the marine ecosystem, their possible toxicity effect on the aquatic biosphere is yet undetermined. Thus, Christen et al. [79] investigated the cytotoxicity of the biocidal disinfectant TAS barquat and benzalkonium chloride (BAC) in human hepatoma cell line (Huh7) and *Danio rerio* liver cells (ZFL). The half-maximum effective concentration ( $EC_{50}$ ) value of BAC in both cells was  $14.23 \mu\text{g/mL}$  in Huh7 cells and  $82 \mu\text{g/mL}$  in ZFL, which was slightly lower compared to the  $EC_{50}$  value of barquat at  $3.4 \mu\text{g/mL}$  in Huh7 cells and  $1.19 \mu\text{g/mL}$  in ZFL. The difference in cytotoxicity of the two substances was clarified by their various modes of action. Evidently, long alkyl chains TAS can penetrate the cell membrane and interfere with the physical and biochemical properties of the cells. The presence of charged nitrogen on the cell membrane surface disrupted the voltage distribution.

Additionally, Duque-Benitez et al. [80] prepared three TAS series, which include (i) halomethylated TAS (series I), (ii) non-halogenated TAS (series II), and (iii) halomethylated choline analog (series III), with the presence of halogen in place of one of the hydrogens and studied the impact of the chain length. The cytotoxicity of the three TAS series was then evaluated *in vitro* against human promonocytic cells U-937 cells. Based on the results, all three TAS series demonstrated high-level cytotoxicity in U-937 cells with  $LC_{50}$  values varying between 21 and  $45 \mu\text{g/mL}$ . The iodinated TAS also recorded high cytotoxicity with the  $LC_{50}$  value range of  $9\text{--}46 \mu\text{g/mL}$ . Surprisingly, a proportional study on *N*-iodomethyl and *N*-chloromethyl TAS indicates the opposite impact of chlorine with respect to the iodine atom compared to other intracellular amastigotes and axenic despite similar toxicity effects in terms of the tether chain length. Eventually, the effect of chain expansion on the cytotoxicity level is more responsive when the iodine atoms appeared in the cationic ammonium head instead of chlorine atoms. On the other hand, Inacio et al. [81] employed the C2BBel columnar epithelial cell line to examine the cytotoxicity of various decyltrimethylammonium bromide ( $C_{10}\text{TAB}/[\text{N}_{1,1,1,10}^+][\text{Br}^-]$ ) compounds. While the microbicidal action of TAS has been discovered for some time, the precise processes underlying it has not been well-understood except for the fact that the membrane charge neutralized and degraded the bacterial membranes at greater doses. As a result, the therapeutic properties of TAS were assessed by comparing its toxic effects and bactericidal activity on mammalian polarized epithelial cells.

The varying toxicity trends in prokaryotic and eukaryotic cells imply the distinct mechanisms of TAS-induced toxicity. For instance, the toxicity rating of the C2BBel cell line was  $C_{12}\text{PB} \approx C_{12}\text{BZK} > C_{12}\text{TAB}/[\text{N}_{1,1,1,12}^+][\text{Br}^-]$ , which was consistent with other mammalian epithelial polarized cells in prior findings. Furthermore, the membrane potential within the plasma membrane of eukaryotic cells was higher than that of prokaryotic cells. Consequently, cationic surfactant adsorption would occur more often on bacterial membranes. On the contrary, the insertion into, translocation across, and rupture of the membrane is more difficult in polarized epithelial cells due to the presence of cholesterol, which is not present in the bacterial membrane. Under a similar TAS-containing aqueous phase, the surfactant concentration at the reaction site(s) in mammalian cells would be lower given the larger total membrane surface and overall size of mammalian cells compared to that of bacteria, thus, possibly contributing to their minimal toxicity level.

Furthermore, Basilico et al. [83] investigated the potential cytotoxicity *in vitro* of a newly developed lipophilic TAS class with an eight-carbon lipophilic electron-rich polyconjugate at the nitrogen atom. The lipophilicity and electronic density of the compound were further modified through the insertion of  $C_{12}\text{--}C_{18}$  saturated alkyl chain and methyl-benzyl substituents. The cytotoxicity of the synthesized TAS was assessed using a human microvascular endothelial cell line (HMEC-1), while the MTT assay was employed to determine cell proliferation. The results revealed that all drugs were safe when applied to the human cell line with the selectivity index ranging from 5.99 to  $22.09 \mu\text{M}$ . Surprisingly, the most potent chemicals were also the least harmful, indicating that they specifically target parasitoid red blood cells. It was assumed that these compounds hindered the transport of choline since their structural criteria for anti-plasmodial action (lipophilicity and polar head around nitrogen) were comparable to those of the pre-identified TAS derivatives.

Generally, gemini TAS surfactants contain two cationic head groups linked to the spacer and two hydrophobic alkyl chains that enhanced the interfacial properties, including additional miscellaneous aggregate morphologies, smaller critical micelle concentrations (CMCs), stronger solubilizing ability, and improved surface activity, compared to a single chain TAS. Previously, a sequence of gemini TAS surfactants with different methylene spacers and chain lengths was synthesized and subjected to a cytotoxicity test using

C6 cells and human embryonic renal cell lines HEK29360. Interestingly, when exposed to the least concentration of these surfactants, the activity of the treated cells was significantly greater than that of untreated cells (control). The hormesis effect was explained by the enhancement of low-concentration drugs and the inhibition of high-concentration drugs. The  $IC_{50}$  values of the gemini TAS surfactants with the same spacer chain length were roughly consistent with the following trend: 12-s-12 > 14-s-14 > 16-s-16, which refers to the hydrophobicity of monomeric species in the surfactants. Similarly, the CMC values for these surfactants in pure water are as follows: 12-s-12 > 14-s-14 > 16-s-16, indicating an increase in hydrophobicity with the increasing length of the alkyl chain. The higher cytotoxicity of the longer chain-length gemini TAS surfactant partly constitutes the higher hydrophobicity, which allows greater contact of the surfactant with the plasma membrane.

The synthesis of new quaternary ammonium methacrylate (QAMs), 2-dimethylamino ethyl methacrylate (DMAEMA) was reported by Li et al. [84] through the addition of tertiary amines to organo-halides with varying chain lengths. The cytotoxicity test was then performed on the developed QAMs using human gingival fibroblasts (HGF) and Odontoblast-like MDPC-23 mice cells. According to findings, the cell viability still prevailed when exposed to QAMs at 0.5 g/mL. Moreover, the cell viability of 2-hydroxyethylmethacrylate (HEMA) and triethylene glycol dimethacrylate (TEGDMA) matched that of the control media without monomer. The viability of HGF and odontoblast-like cells was reduced as the monomer content in the medium increased. The findings showed that the increase in both monomer concentration and chain length influenced the increase in cytotoxicity.

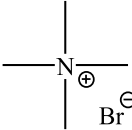
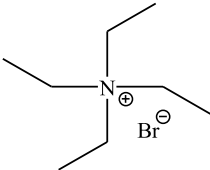
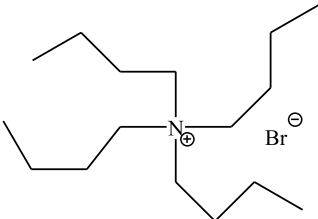
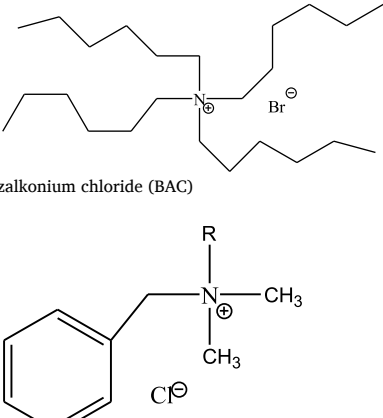
Apart from the MTT assay, previous studies have employed the *in vitro* cytotoxicity of TAS using other methods (Table 1; section other assays). Previously, Dzhemileva et al. [85] demonstrated the first large-scale cytotoxic analysis of various types of TAS, including cholinium and ammonium derivatives. A total of seven human cell lines (HEK293, A2780, U937, A549, K562, HL60, and Jurkat) were employed to identify the relationship between the structural components of TAS and the cytotoxicity level using the concentration required to decrease the proliferative activity by 2-fold values ( $CC_{50}$ ). The test substances were evaluated for cytotoxicity using PrestoBlue Cell Viability Reagent. Based on the findings, the cytotoxic impact of the alkyl chain length in the TAS was nearly independent of the type of cation and anion TAS, including the type affected of cell lines. The presence of an oxygen atom in the side alkyl chain showed no significant effect on the cytotoxicity of TAS.

For instance, Erfurt et al. [86] applied the WST-1 test to assess the cytotoxicity of ILs in rat leukemia IPC-81 cell line. The phase-transfer catalysis (PTC) method was proposed to produce 2-chloro-1,3-butadiene (chloroprene) using D-glucose-based TAS as the catalyst. Then, bromide-based TAS with  $R_1=CH_3C_{12}H_{25}$  and  $C_{16}H_{33}$  were selected to evaluate the lipophilicity of the produced salts on their cytotoxicity. Based on the  $EC_{50}$  results, the  $[GlcO(CH_2)_2N(CH_3)_3]Br$  TAS showed no cytotoxic effect on the viability of the IPC-81 cell line up to a concentration of 584 mol/L. However, the  $EC_{50}$  values for other compounds with longer side chains at a range of 9.5–85.1 mol/L indicated a considerable cytotoxic effect. Additionally, the  $EC_{50}$  value of the TAS derivative with a dodecyl side chain and linked with bromide anion was an order of magnitude greater than that of the derivative with a hexadecyl side chain. Interestingly, the toxicity of the  $[GlcO(CH_2)_2N(CH_3)_2(C_{16}H_{33})]$  cation in combination with either bromide or bis(trifluoromethanesulfone)imide ( $NTf_2$ ) was similar. The increased cytotoxicity along with the extension of the alkyl substituent in this study demonstrated the strong correlation between the cytotoxicity and hydrophobicity of the TAS. The result shows the significant reduction of cytotoxicity when more hydrophilic D-glucose is used to replace the phenyl ring.

The minimum concentration required to cause 50 % cell death (MTS assay) and the minimum concentration required to release 50 % LDH from cells (LDH assays) have also been employed to assess the cytotoxicity of TAS. Perinelli et al. [70] performed the MTS and LDH assays on human epithelial cell lines, namely Caco-2 (intestinal) and Calu-3 (airway) to analyse and compare the cytotoxicity profiles of TAS derived from methionine and leucine and esterified with fatty acids at different chain lengths ( $C_{10}$ ,  $C_{12}$ , and  $C_{14}$ ) with commercial BAC. The MTS colorimetric assay assessed the cell viability of the synthesized TAS at various concentrations, while the LDH method evaluated the impact of TAS on membrane disruption as a responsive and relevant test based on the materials.  $EC_{50}$  results were then calculated based on the hydrophobic value of the TAS, which is largely influenced by the length of the hydrocarbon chain. According to the findings, the  $EC_{50}$  values decreased as the hydrophobicity increased. The LDH assay recorded a marginally higher value, while no significant discrepancies in cytotoxicity were observed between the two cell lines. Besides the expected interaction between cytotoxicity and hydrophobicity, the study also identified the relationship between  $EC_{50}$  values (from both MTS and LDH assays) were much lower than those of CMC values, demonstrating the ability of mammalian epithelial cells to extract and solubilize phospholipids, subsequently contributing to the development of cell membrane destruction and mixed micelles.

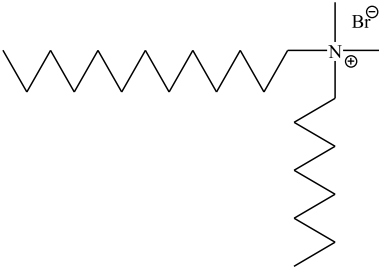
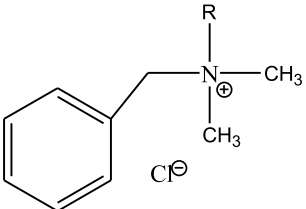
Furthermore, Inacio et al. [88] studied the cell membrane permeabilization using the lactate dehydrogenase (LDH) leakage assay in columnar epithelial (MDCK) cell line *in vitro* exposed to ecytrimethyl ammonium bromide ( $C_{10}TAB/[N_{1,1,1,1,10}^+][Br^-]$ ) at different concentrations for 3 h. The cell viability of the MDCK started to decline at  $C_{10}TAB$  concentrations of 1.3 mM (CMC/30) with the  $LD_{50}$  at 3.1 mM. Nevertheless, membrane damage only occurred at 2.7 mM (CMC/15) with the  $LD_{50}$  at 3.8 mM. Although the cells eventually died, the membrane leakage was the probable cause of death rather than the direct impact of the TAS. Carpenter et al. [89] also investigated the toxicity of TAS-functionalized silica nanoparticles with and without the presence of nitric oxide (NO) on L929 fibroblast [65]. Fibroblast cells signify the standard benchmark for cytotoxicity tests given their major role in immune response and wound healing. The inclusion of primary amines in control *N*-(6-aminohexyl) aminopropyltrimethoxysilane (AHAP) particles resulted in a considerable toxicity at a higher particle dosage of 6 mg/mL. When 8 mg/mL of methyl QA particles were used, the cytotoxicity was significantly reduced as the primary amines were converted to trimethyl QA groups, which corresponded to the 40% reduction in cell viability. However, an increased in cytotoxicity of the QA-functionalized particles against fibroblasts at their minimum bactericidal concentration (MBC) was observed as the alkyl chain length increased. Accordingly, the fibroblast viability was reduced by 21 % and 86 % when treated with 4 and 16 g/mL BAC, respectively. The detection of harmful effects of particle-bound TAS even at substantially lower BAC concentrations indicates the advantages of particle-bound TAS.

**Table 2**  
*In vitro* genotoxicity assay of TAS.

TAS	Strain/Sel/Organism	Genotoxicity	References
Tetramethylammonium bromide/[N <sub>1111</sub> <sup>+</sup> ][Br <sup>-</sup> ]	<i>Salmonella typhimurium</i>	MI (TA98) = 1.47 ± 0.26 MI (TA100) = 0.90 ± 0.07	[ ]
 Tetraethylammonium bromide [N <sub>2222</sub> <sup>+</sup> ][Br <sup>-</sup> ]	<i>Salmonella typhimurium</i>	MI (TA98) = 1.33 ± 0.28 MI (TA100) = 1.04 ± 0.03	[93]
 Tetrabutylammonium bromide/ [N <sub>4444</sub> <sup>+</sup> ][Br <sup>-</sup> ]	<i>Salmonella typhimurium</i>	MI (TA98) = 1.07 ± 0.21 MI (TA100) = 1.19 ± 0.06	[93]
 Tetrahexylammonium bromide / [N <sub>6666</sub> <sup>+</sup> ][Br <sup>-</sup> ]	<i>Salmonella typhimurium</i>	MI (TA98) = 1.21 ± 0.80 MI (TA100) = 1.09 ± 0.08	[93]
 Benzalkonium chloride (BAC)	<i>D. magna</i> <i>C. dubia</i>	EC <sub>50</sub> = 38.2 μg/L LC <sub>50</sub> = 403.7 μg/L	[94]
Dimethyldioctadecylammonium bromide (DMDODAB)/[N <sub>1,1,18,18</sub> <sup>+</sup> ][Br <sup>-</sup> ]	Primary rat hepatocytes	1 mg/L	[95]

(continued on next page)

Table 2 (continued)

TAS	Strain/Sel/Organism	Genotoxicity	References
 Benzalkonium chloride (BAC)	primary rat hepatocytes	1.0 and 3.0 mg/L	[95]
			

## 2.2. In vitro genotoxicity

*In vitro* cytotoxicity test can also be performed through genotoxicity assays, which involve successive procedures to evaluate induced DNA damage that affects the structure, segregation, or content of DNA and are not essentially related to mutagenicity [90]. As such, three primary endpoints (structural chromosome aberrations, numerical chromosome aberrations, and gene mutation) should be investigated for an appropriate genotoxic analysis. Each event is involved in heritable diseases and carcinogenesis. The standard *in vitro* test battery consists of a bacterial reverse mutation test (OECD TG 471), mammalian chromosomal aberration test (OECD TG 473), mammalian cell mutation test (OECD TG 476) and TG 490 and mammalian cell micronucleus test (OECD TG 487). Any *in vivo* confirmatory continue test must cover the same endpoint, which has achieved positive results [91].

One of the commonly performed genotoxicity tests is the bacteria reverse mutation test (Ames test). The test identifies mutations that are the root cause of several human genetic disorders and play a crucial role in tumour growth and initiation (Table 2). The bacterial strains have different mutations that deactivate the gene engaged in the synthesis of critical amino acids, namely tryptophan (*Escherichia coli*) or histidine (*Salmonella*) so that the strains can only develop in culture media that complement those amino acids. Appropriate mutations include substituting particular base pairs or frameshift mutations triggered by the deletion or inclusion of DNA [92].

Previously, Reid et al. [93] reported the mutagenicity index (MI) of protic ionic liquids (PILs) comprising TAS cations depending on the Ames assay that utilized *Salmonella typhimurium* strain TA100 and TA98. Based on the results, the increasing length of the alkyl side chain on the cation and thereby the lipophilicity increased the MI with the TA98 strain. Despite the presence of a longer aliphatic chain inside its structure compared to other hydroxyl cations in this sample, TAS cation showed varying behaviour, which indicates that hydroxyl groups could minimize the resulting MI of the TAS as a result of the increased alkyl chain length. The inclusion of polar functional groups in TAS cation complexes has been associated with a decline in the reported toxicity, so it is reasonable that the studied mutagenicity similarly decreased.

On the other hand, Lavorgna et al. [94] carried out the acute chronic toxicity and alkaline Comet assay to assess the genotoxicity of TAS on *Ceriodaphnia dubia* and *Daphnia magna* subjected to BAC concentrations. The Comet assay, also known as the single-cell gel electrophoresis assay, identifies strand breaks and alkali-labile sites from the association of multiple toxic intermediates with DNA after being exposed to a broad spectrum of genotoxins, such as UV radiation. The findings indicate a strong initiation of DNA migration with BAC, where the DNA migration was calculated by lesions and DNA single-strand breaks that formed single-strand cracks. The percentage of DNA in tail intensity (%) recorded significant damage on both *D. magna* and *C. dubia* after 24 h of exposure, beginning at 0.4 ng/L. Besides, Ferik et al. [95] published the first study on the genotoxic effects of benzalkonium chloride (BAC) and didecyl dimethyl ammonium chloride (DDAC) in primary rat hepatocytes using the Comet assay. The findings revealed that didecyl dimethyl ammonium bromide (DDAB) (or structurally known as DMDODAB/[N<sup>+</sup><sub>1,18,18</sub>][Br<sup>-</sup>]) exhibited a greater significant impact through the Comet assay compared to that of BAC.

## 2.3. In vivo toxicity studies

Animal studies and established *in vitro* models are frequently employed to assess the possible adverse effects of specific compounds

on human health, domestic pets, and livestock animals [74]. Although the primary goal of toxicity analysis is to determine the harmful health effects of xenobiotics, the approach may be supplemented by more complex biomolecular techniques targeted at elucidating the mechanisms of action of specific compounds. In view of this, laboratory animals have become a significant and well-established instrument to analyse *in vivo* toxicological results of newly developed chemicals and medicinal items. Initially proposed to predict acute systemic toxicity in animals, *in vivo* toxicology analyses have adopted increasingly complex, highly precise, and multispecies techniques with well-defined objectives and experimental methodologies, notably for regulatory testing.

Acute toxicity studies are often conducted as preliminary evaluations for the development of novel substances and to detect the presence of possible toxicity. They are also used as the first analytical tool to determine the harmful impacts of a limited delivery period of a single drug dose. The highly versatile acute toxicity studies have therefore often been applied to evaluate the possible toxicity of ILs. However, the most common side effects of acute toxicity studies are morbidity or mortality. Thus, the conventional method of performing acute oral toxicity studies involves the evaluation of the lethal dose, 50 % (LD<sub>50</sub>), which reflect the dose of ILs that induces mortality, and effective dose, 50 % (ED<sub>50</sub>), which indicate any specified consequence in 50 % of the model species [96]. Acute dermal or inhalation tests are conducted when laboratory animal specimens are intensely exposed to ILs in water, which is also expressed as the concentration of ILs that induces mortality (LC<sub>50</sub>) or other specified impacts (EC<sub>50</sub>) in 50 % of the model species. The outcome of acute toxicity studies does not only establish the toxicity degree of ILs and classify them as hazardous materials but also determine the IL dosages for sub-lethal disinfectant application, evaluate chronic toxicity levels, compare the toxicity among IL members, and assists in collecting low-toxicity ILs for potential applications.

Realizing the high risk of human exposure to TAS, epidemiological findings that associate TAS with allergic infection, and the demand for extensive dermal toxicological evidence, Shane et al. [97] assessed the skin sensitization and irritancy potential of DDAB using a murine model to evaluate its role in the development of allergic infection. The local lymph node assay (LLNA) was utilized to estimate the sensitization capacity at varying concentrations of 0.0625–2 %. Based on the results, DDAB caused major irritancy in female BALB/c mice, as indicated by ear swelling. After four and 14 days of DDAB exposure, a substantial increase in gene expression was reported in the draining lymph nodes (DLN) and ear. The findings demonstrated the potential hypersensitivity and inflammation reactions of DDAB following dermal exposure, which raised questions regarding the impact of exposure duration on the hypersensitivity reactions. Furthermore, Lee et al. [98] evaluated the acute toxicity of BAC on target organs in mice and LD<sub>50</sub> following intratracheal instillation and oral intake prior to the recurrent dosage toxicity test. BAC is a common TAS and has been related to toxic effects on the eyes, skin, and airways. According to the results, most of the mice died within 24 h of oral BAC intake at 400 mg/kg, while none were affected after being exposed to 100 mg/kg after 14 days. Additionally, dose-dependent mortality was observed at 150–300 mg/kg with an increase in the number of dead mice against time. The BALB/c mice were subjected to a single oral dose of BAC and recorded an LD<sub>50</sub> of 241.7 mg/kg. After the intratracheal therapy, the LD<sub>50</sub> was reduced to 8.5 mg/kg, indicating that the lung could be the primary source of toxicity.

*In vivo* toxicity on TAS also include the use of invertebrates with *D. magna* as the most frequently studied invertebrate [99]. Recently, Mori et al. [100] performed an acute toxicity test of tetraalkyl ammonium cation involved in the process of making liquid crystal display of thin-film transistors assessed with batteries and electrolytes, namely TMAH, TEAA, TBAH, and NH<sub>4</sub>Cl, using a 24-hr *D. magna* immobilization test (Daphtox kit F). It was found that compounds containing larger alkyl groups, including TBAH and TEAA, recorded greater toxicity to *D. magna*, while NH<sub>4</sub>Cl achieved the lowest toxicity level. A unique synergistic action of iodide was also observed compared to other halide salts namely, bromide, chloride, and fluoride. Longer alkyl chains of TAS ions, such as TEAA and TBAH, were more toxic than TMAH in the *D. magna* immobilization test. Other related studies have also examined the toxicity of TAS *in vivo* against vertebrates is limited. Li et al. [101] reported the toxicity of three quaternary ammonium based ILS 1-hydroxyethyl-3-methylimidazolium tetrafluoroborat ([HOEMIm]BF<sub>4</sub>), 1-methoxyethyl-3-methylimidazolium tetrafluoroborat ([MOEMIm]BF<sub>4</sub>), 1-aminoethyl-3-methylimidazolium tetrafluoroborate ([C<sub>2</sub>NH<sub>2</sub>MIm]BF<sub>4</sub>) on zebrafish. Based on the acute toxicity test, the median concentration after 96 h (LC<sub>50</sub>) of the three ILS in zebrafish was 3086.7 mg/L, 2492.5 mg/L, and 143.8 mg/L, respectively. In a separate study, Mori et al., 2015 [102] investigated the TAS toxicity of Medaka fish (*Oryzias latipes*) following the OECD 203 test procedure (OECD, 1992). The TAS exposure showed a severe impact on the zebrafish growth with the 96 h of death test exposure recording an LC<sub>50</sub> value of 154 mg/L.

### 3. Insight and conclusions

This review presented a significant number of studies with varying views of the toxicity effects and the safe use of TAS on human health and a broad range of living organisms as well as the environment. While certain researchers claimed that TAS materials are biocompatible in various biomedical investigations, others have refuted the claim by demonstrating the undesirable biological reactions of TAS, including cytotoxicity [103–109]. The contradicting findings could have arisen due to the notable differing variables in each study, including different study organizations, specific cellular or animal models, and different physicochemical characterizations of TAS. Nevertheless, the performance and competitiveness of many science-based and industrial processes, including nanotechnology, organic synthesis, electrochemistry, catalysis, and analytical chemistry, have increased as a result of the recycling capabilities of TAS.

Therefore, researchers are compelled to develop new approaches to exploit the non-volatile properties of TAS, which are not shown by conventional media. The *in vivo* biocompatibility of TAS for human consumption or other biomedical applications must be addressed with an in-depth toxicity analysis. Furthermore, since this material has emerged as important component in the solar photovoltaic industry especially perovskite solar cell which foresee extremely fast progress by tri-fold its performance in just ten years, detailed research on the possible hazards of perovskite solar cell's materials to human health and the environment is required.

Addressing the potential toxicity of PSCs is crucial, and numerous life cycle analysis (LCA) studies have been conducted to evaluate



their environmental impacts precisely [110]. While the leaching of Pb from PSC panels during their lifespan results in a low contamination level compared to background values of Pb in urban areas, anticipating the environmental impact of the abundance of obsolete PSCs at the end of their shelf life is imperative. This remains a critical concern, especially with the widespread implementation of commercial PSC products. Therefore, proactive attention should be given to urban mining approaches, incorporating waste recycling, resource recovery, and circular technological solutions. As of now, solar cells, including PSC, are regulated under waste electrical and electronic equipment guidelines in the EU and China, which could potentially accelerate recycling and recovery initiatives [111]. The composition ratio of PSC (in molar ratio) consists of approximately 60 % ETL, 38 % HTM, and 2 % perovskite structure [112]. Although TAS is estimated to contribute ~1% to the composition, this figure does not fully reflect the diverse applications of TAS as a precursor, additive, solvent, interfacial layer, and protective layer in various procedures for preparing high-performance PSC devices. On the contrary, a majority of PSC components can be easily removed through dissolution in polar organic solvents, alkaline aqueous solutions, and ionic eutectic solvents, presenting promising prospects for industrializing the recycling and reuse of TCO/ETL substrates from PSCs. However, the inevitable generation of waste and end-of-life devices poses serious environmental concerns. Therefore, proactive development of recycling and recovery technologies for perovskite solar cells, where individual components in the perovskite can be recycled and recovered using various physical and chemical methods, is necessary. For instance, precious metal contacts such as Aurum (Au), Argentum (Ag), and Platinum (Pt) can be recovered through electrochemical extraction. Subsequently, purification and recycling processes can be applied to the HTM component and the perovskite layer, utilizing methods such as dissolution, solvent extraction, column chromatography, precipitation, and crystallization. Washing, sonication, and annealing methods can be employed for the ETL and FTO components [110]. As mentioned earlier, TAS can be recovered and purified using the same processes applied to the HTM component and the perovskite layer in the perovskite mixture. Despite the remarkable versatility of TAS in various aspect in solar cells application, it is imperative to note that regulatory bodies often mandate cytotoxicity testing as an integral component of safety assessments. This is particularly crucial when considering the commercial application of TAS compounds. Besides, the extensive application of TAS has raised the risk of harmful chemical leakage into the atmosphere. Regardless of the green properties, the ecotoxicity of freshly synthesized TAS for industrial application should be determined since various reports have shown the potential harm of TAS on the climate. Interestingly, the rapid advancement of green technology facilitates the innovative development of TAS with biodegradable and environmentally friendly features. The toxicity test on bio-based TAS has been recognized as a significant step toward developing more sustainable, biodegradable, and ecologically beneficial TAS derivatives. The utilization of natural and bioactive chemicals, such as fatty acids, amino acids, choline, and other natural acids, has sparked a new interest in the development of bio-based TAS. Hence, it is critical to establish a standard guideline that regulates the synthesis of non-toxic and biodegradable materials from sustainable sources, such as choline, sugars, bicyclic monoterpene moiety derivatives, and amino acids.

To the best of the author's knowledge, only a few research on the toxicity of bio-based TAS for solar industry usage, mainly TAS produced from fatty acids, have been reported so far. Conventional TAS toxicity information used in solar cells is only obtained from previous studies and other sources, for example TBACl,  $IC_{50}$  (Cell line) = 1.79–27.47 mM [85], TBAI,  $LD_{50}$  Oral (rat) = 1990 mg/kg and  $LD_{50}$  Oral (mouse) = 112 mg/kg [113]. Fatty acids are formed through the hydrolysis of triacylglycerol molecules and are naturally found in vegetable oils, such as soy and sunflower oils. They also cause acidity and off-flavour in crude vegetable oils. Because of their renewal resources, the synthesis and usage of TAS ionic liquids from biobased are receiving more attention. Taken together, this review highlights the need to determine the toxicity and hazards of new materials prepared from new sources so that they are not harmful to human health and do not pollute the environment.

### CRedit authorship contribution statement

**N.M. Mustafa:** Writing – review & editing, Writing – original draft, Visualization, Resources, Investigation, Formal analysis. **F.N. Jumaah:** Writing – review & editing, Methodology, Investigation, Conceptualization. **N.A. Ludin:** Validation, Supervision, Resources, Project administration, Funding acquisition. **N.H. Hassan:** Visualization, Validation, Supervision, Software. **M. Akhtaruzzaman:** Supervision, Formal analysis, Data curation. **A. Ahmad:** Writing – review & editing, Resources, Funding acquisition, Data curation. **K. M. Chan:** Writing – review & editing, Writing – original draft, Supervision, Methodology, Investigation, Formal analysis. **M.S. Su'ait:** Writing – review & editing, Validation, Supervision, Methodology, Funding acquisition.

### Declaration of competing interest

The authors declare that they have no known competing financial interests or personal relationships that could have appeared to influence the work reported in this paper.

### Acknowledgement

This research was funded by the Malaysia Ministry of Higher Education (MOHE) through Fundamental Research Grant Scheme (FRGS) under the grant number FRGS/1/2022/TK0/UKM/02/15. The authors thank the Universiti Kebangsaan Malaysia (UKM), and Solar Energy Research Institute (SERI) for allowing this research to be carried out. Appreciation to PhD Scholarship, Hadiah Latihan Persekutuan (HLP) support to Ts. Nur Maizura Mustafa by Public Service Department of Malaysia (JPA).

## References

- [1] N.V. Plechkova, K.R. Seddon, Applications of ionic liquids in the chemical industry, *Chem. Soc. Rev.* 37 (2008) 123–150.
- [2] B.E. Brycki, I.H. Kowalczyk, A.M. Szulc, et al., Quaternary alkylammonium salts as cleaning and disinfectant agents, *Tenside, Surfactants, Deterg.* 55 (2018) 432–438.
- [3] H. Kiyokawa, H. Tokutomi, S. Ishida, et al., Thermal energy storage performance of tetrabutylammonium acrylate hydrate as phase change materials, *Appl. Sci.* 11 (2021) 4848.
- [4] Fatimah Najirah Jumaah, Review of non-crystalline and crystalline quaternary ammonium ions: classification, structural and thermal insight into tetraalkylammonium ions, *J. Mol. Liq.* 63 (2023) 1–25.
- [5] R. Pandey, S. Bhattarai, K. Sharma, et al., Halide composition engineered a non-toxic perovskite-silicon tandem solar cell with 30.7% conversion efficiency, *ACS Appl. Electron. Mater.* 5 (2022) 5303–5315.
- [6] S. Chauhan, M. Kaur, K. Singh, et al., Micellar and antimicrobial activities of ionic surfactants in aqueous solutions of synthesized tetraalkylammonium based ionic liquids, *Colloids Surf. A Physicochem. Eng. Asp.* 535 (2017) 232–241.
- [7] A. Ciccioli, R. Panetta, A. Luongo, et al., Stabilizing lead halide perovskites with quaternary ammonium cations: the case of tetramethylammonium lead iodide, *Phys. Chem. Chem. Phys.* 21 (2019) 24768–24777.
- [8] F.N. Jumaah, N.M. Mustafa, N.N. Mobarak, et al., Bio-based quaternary ammonium salt as an electrolyte for dye-sensitized solar cells, *Electrochim. Acta* 472 (2023) 143383.
- [9] R. Mooney, M. Masala, T. Martial, et al., Alkyl-carbon chain length of two distinct compounds and derivatives are key determinants of their anti-Acanthamoeba activities, *Sci. Rep.* 10 (2020) 6420.
- [10] R. Méreau, B. Grignard, A. Boyaval, et al., Tetrabutylammonium salts: cheap catalysts for the facile and selective synthesis of  $\alpha$ -alkylidene cyclic carbonates from carbon dioxide and alkynols, *ChemCatChem* 10 (2018) 956–960.
- [11] J. Zackiewicz, A. Jakubowska, E. Grabinska-Sota, Toxicity of quaternary ammonium ionic liquids to aquatic organisms, *Chemik* 69 (2015) 477–484.
- [12] R. Manivannan, S.N. Victoria, Preparation of chalcogenide thin films using electrodeposition method for solar cell applications – A review, *Sol. Energy* 173 (2018) 1144–1157.
- [13] J.C. Malaquias, M. Steichen, M. Thomassey, et al., Electrodeposition of Cu-In alloys from a choline chloride based deep eutectic solvent for photovoltaic applications, *Electrochim. Acta* 103 (2013) 15–22.
- [14] S. Kim, N.G. Yoon, B. Jana, et al., Quaternary ammonium-based mitochondria targeting anticancer agents with high water solubility, *Bull. Kor. Chem. Soc.* 43 (2022) 391–395.
- [15] J.M. Boyce, Quaternary ammonium disinfectants and antiseptics: tolerance, resistance and potential impact on antibiotic resistance, *Antimicrob. Resist. Infect. Control* 12 (2023) 1–14.
- [16] J.D.B. Featherstone, Dental restorative materials containing quaternary ammonium compounds have sustained antibacterial action, *J. Am. Dent. Assoc.* 153 (2022) 1114–1120.
- [17] A. Góra, L. Tian, S. Ramakrishna, et al., Design of novel perovskite-based polymeric poly(L-lactide-co-glycolide) nanofibers with anti-microbial properties for tissue engineering, *Nanomaterials* 10 (2020) 1–19.
- [18] S. Banerjee, R.N. Gayen, Tetramethylammonium based lead free perovskite active layer for solar cell application, *Ceram. Int.* 45 (2019) 17438–17441.
- [19] M. Shahiduzzaman, K. Yamamoto, Y. Furumoto, et al., Viscosity effect of ionic liquid-assisted controlled growth of  $\text{CH}_3\text{NH}_3\text{PbI}_3$  nanoparticle-based planar perovskite solar cells, *Org. Electron.* 48 (2017) 147–153.
- [20] S. Lou, Z. Zhou, T. Xuan, et al., Chemical transformation of lead halide perovskite into insoluble, less cytotoxic, and brightly luminescent  $\text{CsPbBr}_3/\text{CsPb}_2\text{Br}_5$  composite nanocrystals for cell imaging, *ACS Appl. Mater. Interfaces* 11 (2019) 24241–24246.
- [21] S. Kotsyuda, A. Wiesner, S. Steinhauer, et al., Synthesis and structural characterization of tetraalkylammonium salts of the weakly coordinating anion  $[\text{Al}(\text{OTeF}_5)_4]^-$ , *Z. Anorg. Allg. Chem.* 647 (2021) 200–203.
- [22] M. Benkova, O. Soukup, L. Prchal, et al., Synthesis, antimicrobial and lipophilicity-activity dependence of three series of dichained N-alkylammonium salts, *ChemistrySelect* 4 (2019) 12076–12084.
- [23] P. Anastasio, T. Del Giacco, R. Germani, et al., Structure effects of amphiphilic and non-amphiphilic quaternary ammonium salts on photodegradation of Alizarin Red-S catalyzed by titanium dioxide, *RSC Adv.* 7 (2017) 361–368.
- [24] S.V. Sapozhnikov, A.E. Sabirova, N.V. Shtyrlin, et al., Design, synthesis, antibacterial activity and toxicity of novel quaternary ammonium compounds based on pyridoxine and fatty acids, *Eur. J. Med. Chem.* (2020) 113100.
- [25] B. Yoo, B. Jing, S.E. Jones, et al., Molecular mechanisms of ionic liquid cytotoxicity probed by an integrated experimental and computational approach, *Sci. Rep.* 6 (2016) 2–8.
- [26] B.I. Andreica, X. Cheng, L. Marin, Quaternary ammonium salts of chitosan. A critical overview on the synthesis and properties generated by quaternization, *Eur. Polym. J.* 139 (2020) 110016.
- [27] H. Kebaili, A. Pérez de los Ríos, M.J. Salar-García, et al., Evaluating the toxicity of ionic liquids on *Shewanella* sp. for designing sustainable bioprocesses, *Front Mater* 7 (2020) 578411.
- [28] F. Bureš, Quaternary ammonium compounds: simple in structure, complex in application, *Top. Curr. Chem.* 377 (2019) 1–21.
- [29] Y. Shynkarenko, M.I. Bodnarchuk, C. Bernasconi, et al., Direct synthesis of quaternary alkylammonium-capped perovskite nanocrystals for efficient blue and green light-emitting diodes, *ACS Energy Lett.* 4 (2019) 2703–2711.
- [30] S. Ghosh, T. Singh, Role of ionic liquids in organic-inorganic metal halide perovskite solar cells efficiency and stability, *Nano Energy* 63 (2019) 103828.
- [31] H. Kim, S.U. Lee, D.Y. Lee, et al., Optimal interfacial engineering with different length of alkylammonium halide for efficient and stable perovskite solar cells, *Adv. Energy Mater.* 9 (2019) 1902740.
- [32] A. Bouich, J. Marí-Guaita, B. Sahaoui, et al., Tetrabutylammonium (TBA)-Doped methylammonium lead iodide: high quality and stable perovskite thin films, *Front. Energy Res.* 10 (2022) 1–10.
- [33] I. Poli, S. Eslava, P. Cameron, Tetrabutylammonium cations for moisture-resistant and semitransparent perovskite solar cells, *J Mater Chem A Mater* 5 (2017) 22325–22333.
- [34] H. Li, S. Yang, S. Gong, et al., Perovskite films with a sacrificial cation for solar cells with enhanced stability based on carbon electrodes, *J. Alloys Compd.* 797 (2019) 811–819.
- [35] L. Chao, Y. Xia, B. Li, et al., Room-temperature molten salt for facile fabrication of efficient and stable perovskite solar cells in ambient air, *Chem* 5 (2019) 995–1006.
- [36] S. Bhattarai, M.K.A. Mohammed, J. Madan, et al., Performance improvement of perovskite solar cell design with double active layer to achieve an efficiency of over 31%, *Sustainability* 15 (2023) 13955.
- [37] P.R. Yan, W.J. Huang, S.H. Yang, Incorporation of quaternary ammonium salts containing different counterions to improve the performance of inverted perovskite solar cells, *Chem. Phys. Lett.* 669 (2017) 143–149.
- [38] M. Shahiduzzaman, L. Wang, S. Fukaya, et al., Ionic liquid-assisted MAPbI<sub>3</sub> Nanoparticle-seeded growth for efficient and stable perovskite solar cells, *ACS Appl. Mater. Interfaces* 13 (2021) 21194–21206.
- [39] F. Zhang, H. Lu, J. Tong, et al., Advances in two-dimensional organic-inorganic hybrid perovskites, *Energy Environ. Sci.* 13 (2020) 1154–1186.
- [40] J. Carrillo, A. Guerrero, S. Rahimnejad, et al., Ionic reactivity at contacts and aging of methylammonium lead triiodide perovskite solar cells, *Adv. Energy Mater.* 6 (2016) 1–22.
- [41] M.K.A. Mohammed, A.K. Al-Mousoi, S.M. Majeed, et al., Stable hole-transporting material-free perovskite solar cells with efficiency exceeding 14% via the introduction of a malonic acid additive for a perovskite precursor, *Energy Fuel.* 36 (2022) 13187–13194.

- [42] H. Zhang, F. Ye, W. Li, et al., Bright perovskite light-emitting diodes with improved film morphology and reduced trap density via surface passivation using quaternary ammonium salts, *Org. Electron.* 67 (2019) 187–193.
- [43] X. Zheng, B. Chen, J. Dai, et al., Defect passivation in hybrid perovskite solar cells using quaternary ammonium halide anions and cations, *Nat. Energy* 2 (2017) 17102.
- [44] A. Góra, L. Tian, S. Ramakrishna, et al., Design of novel perovskite-based polymeric poly(L-lactide-co-glycolide) nanofibers with anti-microbial properties for tissue engineering, *Nanomaterials* 10 (2020) 1–19.
- [45] S. Liu, M. Gonzalez, C. Kong, et al., Synthesis, antibiotic structure–activity relationships, and cellulose dissolution studies of new room-temperature ionic liquids derived from lignin, *Biotechnol. Biofuels* 14 (2021) 1–10.
- [46] R. Sasi, T.P. Rao, S.J. Devaki, Bio-based ionic liquid crystalline quaternary ammonium salts: properties and applications, *ACS Appl. Mater. Interfaces* 6 (2014) 4126–4133.
- [47] P. Mester, C. Robben, A.K. Witte, et al., FTIR spectroscopy suggests a revised mode of action for the cationic side-chain effect of ionic liquids, *ACS Comb. Sci.* 21 (2019) 90–97.
- [48] J. Theerthagiri, R.A. Senthil, M.H. Buraidah, et al., Effect of tetrabutylammonium iodide content on PVDF-PMMA polymer blend electrolytes for dye-sensitized solar cells, *Ionics* 21 (2015) 2889–2896.
- [49] R.A. Senthil, J. Theerthagiri, J. Madhavan, et al., Performance characteristics of guanine incorporated PVDF-HFP/PEO polymer blend electrolytes with binary iodide salts for dye-sensitized solar cells, *Opt. Mater.* 58 (2016) 357–364.
- [50] M. Zhao, J. Gao, H. Zhang, et al., Quaternary ammonium compounds promoted anoxic sludge granulation and altered propagation risk of intracellular and extracellular antibiotic resistance genes, *J. Hazard Mater.* 445 (2023) 130464.
- [51] P. Meier, P. Clement, S. Altenried, et al., Quaternary ammonium-based coating of textiles is effective against bacteria and viruses with a low risk to human health, *Sci. Rep.* 13 (2023) 1–13.
- [52] Y. Bi, W. Li, C. Liu, et al., Star-shaped quaternary ammonium compounds with terminal amino groups for rapidly breaking oil-in-water emulsions, *Fuel* 304 (2021) 121366.
- [53] T. Bento de Carvalho, J.B. Barbosa, P. Teixeira, Effectiveness and durability of a quaternary ammonium compounds-based surface coating to reduce surface contamination, *Biology* 12 (2023) 1–11.
- [54] Z. Liu, Z. Yu, X. Cao, et al., An environmentally friendly material for red tide algae removal: performance and mechanism, *Front. Mar. Sci.* 9 (2022) 1–13.
- [55] R.A. Sequeira, M.M. Pereira, P. Vaghela, et al., Sustainable production of quaternary ammonium seaweed polysaccharide salts and their evaluation for seed dressing in agricultural applications, *ACS Agric. Sci. Technol.* 1 (2021) 674–683.
- [56] A.A. Shamsuri, S.N.A.M. Jamil, Application of Quaternary Ammonium Compounds as Compatibilizers for Polymer Blends and Polymer Composites-A Concise Review, *Applied Sciences* 11 (2021) 3167.
- [57] T.G. Osimitz, W. Droege, Quaternary ammonium compounds: perspectives on benefits, hazards, and risk, *Toxicol. Res. Appl.* 5 (2021) 239784732110490.
- [58] R. Ahmad, E. Cho, S. Rakhmat, et al., Characterization of structure isomers of ethylbenzalkyl dimethyl ammonium chlorides and quantification in commercial household disinfectant products, *Environ. Technol. Innov.* 29 (2023) 102979.
- [59] G. Zheng, E. Schreder, S. Sathyanarayana, et al., The first detection of quaternary ammonium compounds in breast milk: implications for early-life exposure, *J. Expo. Sci. Environ. Epidemiol.* 32 (2022) 682–688.
- [60] M. Rayung, M.M. Aung, S.C. Azhar, et al., Bio-based polymer electrolytes for electrochemical devices: insight into the ionic conductivity performance, *Materials* 13 (2020) 838.
- [61] I. Ali, S. Burki, B.M. El-Haj, et al., Synthesis and characterization of pyridine-based organic salts: their antibacterial, antibiofilm and wound healing activities, *Bioorg. Chem.* 100 (2020) 103937.
- [62] O. Melezhyk I, V. Rodik R, V. Iavorska N, et al., Antibacterial properties of tetraalkylammonium and imidazolium tetraalkoxycalix[4]arene derivatives, *Antiinfect Agents* 13 (2015) 87–94.
- [63] P. Makvandi, R. Jamaledin, M. Jabbari, et al., Antibacterial quaternary ammonium compounds in dental materials: a systematic review, *Dent. Mater.* 34 (2018) 851–867.
- [64] I. Alrubaie, A.T. Salim, M.M. Majeed, et al., Synthesis of novel polymer quaternary ammonium salt derived from glucose as a phase transfer catalyst, *Nusantara Biosci.* 14 (2022) 25–33.
- [65] C. Samorì, A. Pasteris, P. Galletti, et al., Acute toxicity of oxygenated and nonoxygenated imidazolium-based ionic liquids to *Daphnia magna* and *Vibrio fischeri*, *Environ. Toxicol. Chem.* 26 (2007) 2379–2382.
- [66] C. Zhang, F. Cui, G. Ming Zeng, et al., Quaternary ammonium compounds (QACs): A review on occurrence, fate and toxicity in the environment, *Sci. Total Environ.* 518–519 (2015) 352–362.
- [67] P.I. Hora, S.G. Pati, P.J. McNamara, et al., Increased use of quaternary ammonium compounds during the SARS-CoV-2 pandemic and beyond: consideration of environmental implications, *Environ. Sci. Technol. Lett.* 7 (2020) 622–631.
- [68] I.P.E. Macário, H. Oliveira, A.C. Menezes, et al., Cytotoxicity profiling of deep eutectic solvents to human skin cells, *Sci. Rep.* 9 (2019) 1–9.
- [69] K. Sharma, V. Sharma, S.S. Sharma, Dye-sensitized solar cells: fundamentals and current status, *Nanoscale Res. Lett.* 13 (2018) 381.
- [70] D.R. Perinelli, D. Petrelli, D. Vllasaliu, et al., Quaternary ammonium leucine-based surfactants: the effect of a benzyl group on physicochemical properties and antimicrobial activity, *Pharmaceutics* 11 (2019) 31248093.
- [71] Y. Jiao, L. Niu, S. Ma, et al., Quaternary ammonium-based biomedical materials: state-of-the-art, toxicological aspects and antimicrobial resistance, *Prog. Polym. Sci.* 71 (2017) 53–90.
- [72] K. Hyla, D. Jama, Grzywacz Aleksandra, et al., Evaluation of the antitumor activity of quaternary ammonium surfactants, *Int. J. Mol. Sci.* 24 (2023) 17237.
- [73] S. Rao, T.N. B, N.K. Preman, et al., Synthesis, characterization, and evaluation of quaternary ammonium-based polymerizable antimicrobial monomers for prosthodontic applications, *Heliyon* 8 (2022) e10374.
- [74] X. Wang, T. Guo, Y. Shu, et al., The anion of choline-based ionic liquids tailored interactions between ionic liquids and bovine serum albumin, MCF-7 cells, and bacteria, *Colloids Surf. B Biointerfaces* 206 (2021) 111971.
- [75] H.G. Zeweldi, A.P. Bendoy, M.J. Park, et al., Tetrabutylammonium 2,4,6-trimethylbenzenesulfonate as an effective and regenerable thermo-responsive ionic liquid drawing agent in forward osmosis for seawater desalination, *Desalination* 495 (2020) 114635.
- [76] R. Ahmadi, B. Hemmateenejad, A. Safavi, et al., Assessment of cytotoxicity of choline chloride-based natural deep eutectic solvents against human HEK-293 cells: a QSAR analysis, *Chemosphere* 209 (2018) 831–838.
- [77] M.O. Karataş, S.A.A. Noma, C. Gürses, et al., Water soluble coumarin quaternary ammonium chlorides: synthesis and biological evaluation, *Chem. Biodivers.* 17 (2020) 202000258.
- [78] X. Xie, W. Cong, F. Zhao, et al., Synthesis, physicochemical property and antimicrobial activity of novel quaternary ammonium salts, *J. Enzym. Inhib. Med. Chem.* 33 (2018) 98–105.
- [79] V. Christen, S. Faltermann, N.R. Brun, et al., Cytotoxicity and molecular effects of biocidal disinfectants (quaternary ammonia, glutaraldehyde, poly (hexamethylene biguanide) hydrochloride PHMB) and their mixtures in vitro and in zebrafish eleuthero-embryos, *Sci. Total Environ.* 586 (2017) 1204–1218.
- [80] S.M. Duque-Benítez, L.A. Ríos-Vásquez, R. Ocampo-Cardona, et al., Synthesis of novel quaternary ammonium salts and their in vitro antileishmanial activity and U-937 cell cytotoxicity, *Molecules* 21 (2016) 27043509.
- [81] Á.S. Inácio, N.S. Domingues, A. Nunes, et al., Quaternary ammonium surfactant structure determines selective toxicity towards bacteria: mechanisms of action and clinical implications in antibacterial prophylaxis, *J. Antimicrob. Chemother.* 71 (2016) 641–654.
- [82] S. Zhang, S. Ding, J. Yu, et al., Antibacterial activity, in vitro cytotoxicity, and cell cycle arrest of gemini quaternary ammonium surfactants, *Langmuir* 31 (2015) 12161–12169.
- [83] N. Basílico, M. Migotto, D.P. Ilboudo, et al., Modified quaternary ammonium salts as potential antimalarial agents, *Bioorg. Med. Chem.* 23 (2015) 4681–4687.
- [84] F. Li, M.D. Weir, H.H.K. Xu, Effects of quaternary ammonium chain length on antibacterial bonding agents, *J. Dent. Res.* 92 (2013) 932–938.



- [85] L.U. Dzhemileva, V.A. D'Yakonov, M.M. Seitkalieva, et al., A large-scale study of ionic liquids employed in chemistry and energy research to reveal cytotoxicity mechanisms and to develop a safe design guide, *Green Chem.* 23 (2021) 6414–6430.
- [86] K. Erfurt, M. Markiewicz, A. Siewniak, et al., Biodegradable surface active D-glucose based quaternary ammonium ionic liquids in the solventless synthesis of chloroprene, *ACS Sustain. Chem. Eng.* 8 (2020) 10911–10919.
- [87] D. Perinelli, G. Palmieri, D. Vllasaliu, et al., Quaternary ammonium surfactants derived from leucine and methionine: novel challenging surface active molecules with antimicrobial activity, *J. Mol. Liq.* 283 (2019) 249–256.
- [88] A.S. Inácio, G.N. Costa, N.S. Domingues, et al., Mitochondrial dysfunction is the focus of quaternary ammonium surfactant toxicity to mammalian epithelial cells, *Antimicrob. Agents Chemother.* 57 (2013) 2631–2639.
- [89] A.W. Carpenter, B.V. Worley, D.L. Slomberg, et al., Dual action antimicrobials: nitric oxide release from quaternary ammonium-functionalized silica nanoparticles, *Biomacromolecules* 13 (2012) 3334–3342.
- [90] C. Pellevoisin, C. Bouez, J. Cotovio, Cosmetic industry requirements regarding skin models for cosmetic testing, in: A.P. Marques, R.L. Reis, R.P. Pirraco, M. Cerqueira (Eds.), *Skin Tissue Models*, UK, Academic Press, London, 1, 2018, pp. 3–37. <https://doi.org/10.1016/C2016-0-00093-1>.
- [91] R. Corvi, F. Madia, In vitro genotoxicity testing—Can the performance be enhanced? *Food Chem. Toxicol.* 106 (2017) 600–608.
- [92] A. Hamel, M. Roy, R. Proudlock, Chapter 4 -The bacterial reverse mutation test, in: R. Proudlock (Ed.), *Genetic Toxicology Testing: A Laboratory Manual*, Elsevier, London, UK, 2016, pp. 79–138. <https://doi.org/10.1016/B978-0-12-800764-8.00004-5>.
- [93] J.E.S.J. Reid, N. Sullivan, L. Swift, et al., Assessing the Mutagenicity of Protic Ionic Liquids Using the Mini Ames Test, *Sustainable Chemical Processes* 3 (2015) 286511821.
- [94] M. Lavorgna, C. Russo, B. D'Abrosca, et al., Toxicity and genotoxicity of the quaternary ammonium compound benzalkonium chloride (BAC) using *Daphnia magna* and *Ceriodaphnia dubia* as model systems, *Environ. Pollut.* 210 (2016) 34–39.
- [95] F. Ferk, M. Mišić, C. Hoelzl, et al., Benzalkonium chloride (BAC) and dimethyldioctadecyl-ammonium bromide (DDAB), two common quaternary ammonium compounds, cause genotoxic effects in mammalian and plant cells at environmentally relevant concentrations, *Mutagenesis* 22 (2007) 363–370.
- [96] J. Ma, X. Li, Methods for Biodegradability and Toxicity Assessment of Ionic Liquid, in: S. Zhang (Ed.), *Encyclopedia of Ionic Liquids*, Springer, Singapore, 2022, p. 16. [https://doi.org/10.1007/978-981-33-4221-7\\_67](https://doi.org/10.1007/978-981-33-4221-7_67).
- [97] H.L. Shane, E. Lukomska, A.B. Stefaniak, et al., Divergent hypersensitivity responses following topical application of the quaternary ammonium compound, didecyldimethylammonium bromide, *J. Immunot.* 14 (2017) 204–214.
- [98] H. Lee, K. Park, Acute toxicity of benzalkonium chloride in Balb/c mice following intratracheal instillation and oral administration, *Environ Anal Health Toxicol* 34 (2019) e2019009.
- [99] C. Wang, Z. Wei, L. Wang, et al., Assessment of bromide-based ionic liquid toxicity toward aquatic organisms and QSAR analysis, *Ecotoxicol. Environ. Saf.* 115 (2015) 112–118.
- [100] I.C. Mori, C.R. Arias-Barreiro, A. Koutsaftis, et al., Toxicity of tetramethylammonium hydroxide to aquatic organisms and its synergistic action with potassium iodide, *Chemosphere* 120 (2015) 299–304.
- [101] W. Li, L. Zhu, Z. Du, et al., Acute toxicity, oxidative stress and DNA damage of three task-specific ionic liquids ([C<sub>2</sub>NH<sub>2</sub>MIm]BF<sub>4</sub>, [MOEMIm]BF<sub>4</sub>, and [HOEMIm]BF<sub>4</sub>) to zebrafish (*Danio rerio*), *Chemosphere* 249 (2020) 126119.
- [102] I.C. Mori, C.R. Arias-Barreiro, A. Koutsaftis, et al., Toxicity of tetramethylammonium hydroxide to aquatic organisms and its synergistic action with potassium iodide, *Chemosphere* 120 (2015) 299–304.
- [103] L.U. Dzhemileva, V.A. D'Yakonov, M.M. Seitkalieva, et al., A large-scale study of ionic liquids employed in chemistry and energy research to reveal cytotoxicity mechanisms and to develop a safe design guide, *Green Chem.* 23 (2021) 6414–6430.
- [104] V.E. Melin, H. Potineni, P. Hunt, et al., Exposure to common quaternary ammonium disinfectants decreases fertility in mice, *Reprod. Toxicol.* 50 (2014) 163–170.
- [105] R.S. Boethling, Environmental fate and toxicity in wastewater treatment of quaternary ammonium surfactants, *Water Research* 18 (1984) 1061–1076.
- [106] N. Baker, A.J. Williams, A. Tropsha, et al., Repurposing quaternary ammonium compounds as potential treatments for COVID-19, *Pharm. Res.* 37 (2020) 32451736.
- [107] T. Santos de Almeida, A. Júlio, N. Saraiva, et al., Choline- versus imidazole-based ionic liquids as functional ingredients in topical delivery systems: cytotoxicity, solubility, and skin permeation studies, *Drug Dev. Ind. Pharm.* 43 (2017) 1858–1865.
- [108] P. Wang, R. Wan, W. Huo, et al., Cytotoxicity, genotoxicity, oxidative stress, and apoptosis in HepG2 cells induced by the imidazole ionic liquid 1-dodecyl-3-methylimidazolium chloride, *Environ. Toxicol.* 35 (2020) 665–672.
- [109] I.R. Benmessaoud, A.L. Mahul-Mellier, E. Horváth, et al., Health hazards of methylammonium lead iodide based perovskites: cytotoxicity studies, *Toxicol. Res.* 5 (2016) 407–419.
- [110] Z. Yue, H. Guo, Y. Cheng, Toxicity of perovskite solar cells, *Energies* 16 (2023) 4007.
- [111] S. Salhofer, B. Steuer, R. Ramusch, et al., WEEE management in Europe and China – a comparison, *Waste Manag.* 57 (2016) 27–35.
- [112] N. Suresh Kumar, K. Chandra Babu Naidu, A review on perovskite solar cells (PSCs), materials and applications, *J. Materiomics* 7 (2021) 940–956.
- [113] PubChem, PubChem Compound Summary for CID 67553, Tetrabutylammonium Iodide, National Center for Biotechnology Information, (2023) (Accessed 3 March 2023).